Idaho
National
Engineering
Laboratory

INEEL/EXT-98-00702

PRELIMINARY DESIGN REPORT FOR SCDAP/RELAP5 LOWER CORE PLATE MODEL

E.W. Coryell (INEEL)

F.P. Griffin (ORNL)

July 1998

Idaho National Engineering and Environmental Laboratory
Lockheed Martin Idaho Technologies
Idaho Falls, Idaho 83415

LOCKHEED MARTIN

DISCLAIMER

DISCLAIMER

Portions of this document may be illegible electronic image products. Images are produced from the best available original document.

Table of Contents

List of Figures

List of Tables

1. INTRODUCTION

The SCDAP/RELAP5 computer code[1] is a best-estimate analysis tool for performing nuclear reactor severe accident simulations. Under primary sponsorship of the U.S. Nuclear Regulatory Commission (NRC), Idaho National Engineering and Environmental Laboratory (INEEL) is responsible for overall maintenance of this code and for improvements for pressurized water reactor (PWR) applications. Since 1991, Oak Ridge National Laboratory (ORNL) has been improving SCDAP/RELAP5 for boiling water reactor (BWR) applications. The RELAP5 portion of the code performs the thermal-hydraulic calculations for both normal and severe accident conditions. The structures within the reactor vessel and coolant system can be represented with either RELAP5 heat structures or SCDAP/RELAP5 severe accident structures. The RELAP5 heat structures are limited to normal operating conditions (i.e., no structural oxidation, melting, or relocation), while the SCDAP portion of the code is capable of representing structural degradation and core damage progression that can occur under severe accident conditions.

SCDAP/RELAP5 severe accident models are currently available to represent (1) the intact structures with associated debris located in the active core region, (2) the intact structures located in the upper plenum above the core, and (3) debris which falls from the core region into the bottom head of the vessel. The SCDAP/RELAP5 core component models (examples are the fuel rod, PWR control rod, and BWR control blade/channel box components) are generally applied to describe structures in the active core region. SCDAP/RELAP5's lower plenum debris model (referred to as the COUPLE module) is generally applied in the hemispherical region of the bottom head. In the current version of SCDAP/RELAP5, the structures located between the bottom head and the bottom of active fuel can only be represented by RELAP5 heat structures (i.e., no SCDAP/RELAP5 severe accident models are available).

At the beginning of a severe accident transient, the reactor vessel coolant level falls until some or all of the core becomes uncovered and begins to heat up. Significant oxidation of the metallic surfaces begins after temperatures exceed about 1000 K, and melting and eutectic liquefaction of the control rod/blade materials occur in the temperature range from about 1200 to 1730 K. During the early phase of a severe accident, this molten metallic material relocates downward and freezes when it encounters a cooler environment. If water is still present in the lower portion of the active core, this solidification will occur within the core region, which is treated by existing SCDAP/RELAP5 mechanistic models. However, once the coolant inventory decreases sufficiently to allow the active core to become completely dry, the molten material relocates below the active core.

Experimental evidence, as well as several analyses, have indicated that amounts of molten metallic material on the order of several metric tons will relocate into and through the core plate region. The relocation of this molten metallic material is expected to occur over an extended period of time (~ 2,000 s). The XR2-1 experiment, a BWR metallic melt relocation experiment conducted at Sandia National Laboratories, indicates that as much as 70% of the metallic relocating material will freeze within the core plate region, at least temporarily, to form non-coherent, localized blockages. During the later phases of the transient, analyses indicate that large amounts (potentially 10's of metric tons) of primarily molten ceramic material will relocate into and through the core plate region. There seems to be little doubt that relocation of material mass of this magnitude and at the temperatures expected, will cause the lower core plate to melt and/or fail if it is retained upon the structure. However, the relative timing of the relocation of this molten metallic and ceramic material is significant. During the time frame of the relocation the core region is

relatively high in temperature, but is in a steam-starved or steam-limited environment. The relocation of the molten material into a pool of coolant which may exist low in the reactor vessel could significantly impact the predicted transient behavior by generating sufficient steam to change the core-region response.

SCDAP/RELAP5 currently assumes that molten material which leaves the core region falls into the lower vessel head without interaction with structural materials. The objective of this design report is to describe the modifications required for SCDAP/RELAP5 to treat the thermal response of the structures in the core plate region as molten material relocates downward from the core, through the core plate region, and into the lower plenum. This has been a joint task between INEEL and ORNL, with INEEL[a] focusing on PWR-specific design, and ORNL[b] focusing upon the BWR-specific aspects.

Chapter 2 describes the structures in the core plate region that must be represented by the proposed model. Chapter 3 presents the available information about the damage progression that is anticipated to occur in the core plate region during a severe accident, including typical SCDAP/RELAP5 simulation results. Chapter 4 provides a description of the implementation of the recommended model and Chapter 5 discusses the testing which could be done to verify the design and implementation of the model.

a. INEEL task specified by Task 11 of Standard Order for DOE Work (SOEW) "Job Code Title: SCDAP/RELAP5 Code Development & Assessment", Job Code Number W6095, December 23, 1997.
b. ORNL task specified by Task 6 of Job Code Number W6581 entitled "SCDAP/RELAP5 BWR Model Development for Severe Accidents".

2. REVIEW OF DESIGNS

A review of currently operating plants was undertaken to categorize plant-specific features. The PWR review has been previously documented[2], while the BWR review is original to this report.

2.1 Pressurized Water Reactor Designs

Representative PWR designs were categorized by vendor, with Final Safety Analysis Reports (FSAR) of the following plants providing design information, except where noted: Three Mile Island-2 (TMI-2)[3] for Babcock and Wilcox, Waterford[4] and Calvert Cliffs[5] for Combustion Engineering, and Braidwood[6] and Zion Station[7] for Westinghouse. The primary purpose of this review was to determine the general types of geometries and materials that must be addressed in the design of the SCDAP/RELAP5 model. It does not address plant specific features necessary to develop detailed input decks for the analysis of individual plants. For example, it is anticipated that the same geometric and phenomenological models would be applicable to the Zion and Surry plants, since both plants are Westinghouse designs. However, because of individual plant differences, such as core and downcomer flow bypass, the input models for these two plants will be noticeably different.

2.1.1 Babcock and Wilcox (B&W)

The lower grid assembly, or lower core support assembly, in TMI-2 supports most of the reactor internal structure. All major components in the lower core support assembly are made of stainless steel. The lower grid assembly, shown in Figure 1, consists of two grid structures, separated by short tubular columns. The two grids are surrounded by a forged, flanged cylinder, with the top flange of the forged cylinder bolted to the lower flange of the core barrel. The upper plate in this assembly is a perforated plate, while the lower structure is a machined forging. The columns transfer loads to the bottom grid, which carries the loads in bending, The core barrel then transmits the load in tension to the reactor vessel. A perforated flat plate located midway between the grid structures aids in distributing coolant flow. Approximate dimensions for components of the lower grid assembly are given in Table 1.

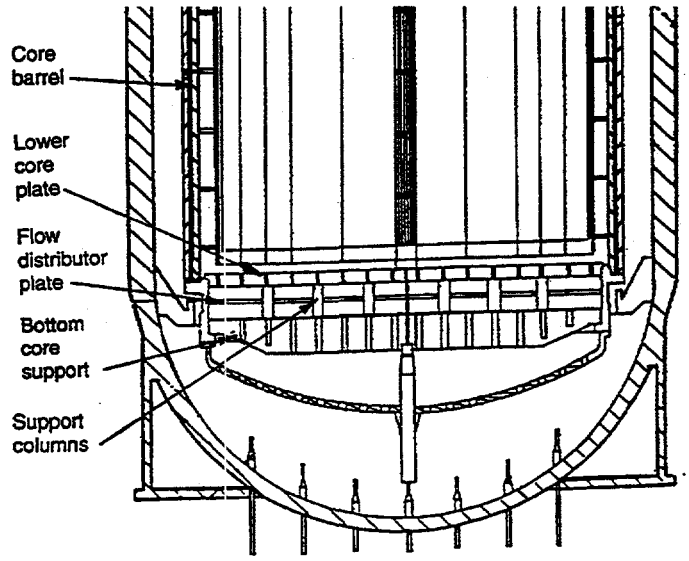

Figure 1. Lower core plate assembly for the TMI-2 plant (B&W).

2.1.2 Westinghouse (W)

The major support for reactor internal structures in the Westinghouse plants is the lower core support assembly, shown in Figure 2. Components which provide support in this assembly include two plates (the lower core plate and bottom core support) which are separated by support columns and surrounded by the core barrel. The support columns provide stiffness and transmit the core load to the core support, which carries the load in bending. The bottom core support, which is the lowest plate in this assembly, is welded to the core barrel, which hangs from a ledge in the reactor head flange. So again, the core barrel carries the dead load of reactor internal structures in tension. Approximate dimensions for components of the lower core support assembly are given in Table 1.

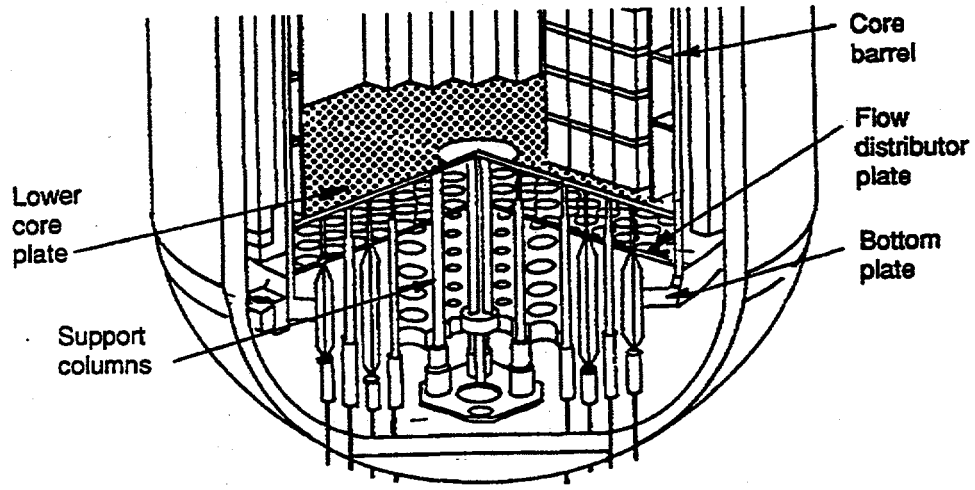

Figure 2. Zion lower core plate assembly (Westinghouse).

Note that in the Westinghouse RESAR design, the core rests directly on the bottom plate (similar to the bottom core support), which hangs from the end of the core barrel. The bottom plate is 44.5 cm. thick in this design.

2.1.3 Combustion Engineering (CE)

Figure 3 shows the lower support assembly which supports reactor internal structures in the Waterford plant. The lower support assembly consists of a lower core plate (directly under the fuel assemblies), support columns, support beams, bottom core support, and surrounding cylinder, all made of Type 304 stainless steel. Loads to the lower core plate are transmitted through the support columns to the support beams. The support beams transform support column (point) loads to line loads on the bottom core support. The bottom core support carries the line loads in bending, transmitting the load to the core barrel, which carries it in tension. Approximate dimensions for components of the lower core support assembly

are given in Table 1.

Table 1. Approximate dimensions for components in lower core support assemblies.

Generic Name		B&W	W	CE
Lower Core Plate	*Diameter (cm)*	*356*	*373*	*363*
	Thickness (cm)	*18.4*	*5.1*	*5.1*
Bottom Core Support	*Diameter (cm)*	*356.*	*381*	*363*
	Thickness (cm)	*34.3*	*53.3*	*8.9*

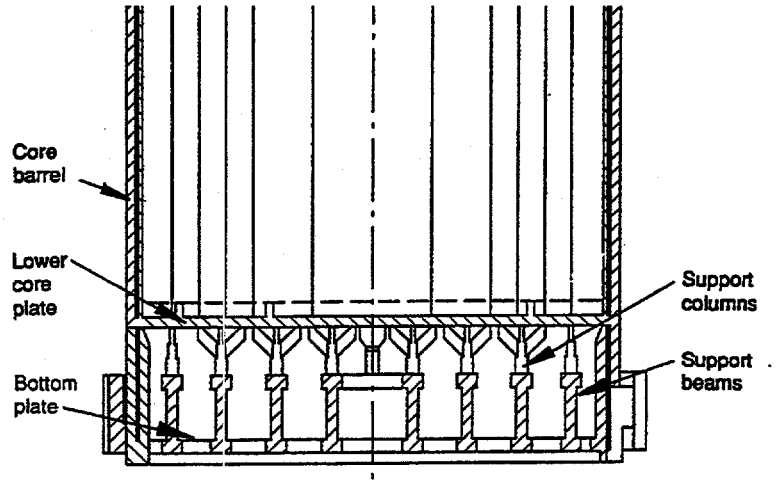

Figure 3. Waterford lower core plate assembly (Combustion Engineering).

2.2 Boiling Water Reactor Designs

The core plate in a BWR separates the core region from the lower plenum as shown in Figure 4. The primary functions of the core plate are (1) to provide lateral (but not vertical) support for the bottom of the fuel assemblies and (2) to provide a barrier that forces most of the upward-flowing coolant into the fuel assemblies. Without the core plate, the coolant would travel the path of least resistance outside the fuel assemblies in the interstitial region.

The weight of the core is supported by the bottom head (except for about 3% of the assemblies at the periphery of the core that are supported directly by the core plate). A group of four fuel assemblies sits on top of a fuel support piece which rests on top of a control rod guide tube. Each control rod guide tube is welded to the bottom head via a control rod drive (CRD) housing and a stub tube. Holes near the tops of the control rod guide tubes align with flow orifices in the fuel support pieces to provide coolant flow paths from the lower plenum into the bottom of each fuel assembly.

A more detailed drawing of a BWR core plate is provided in Figure 5. The core plate is fabricated from a 5.08-cm (2-in.) thick piece of stainless steel with large holes [27.94-cm (11-in.) diameter on 30.48-cm (12-in.) centers] to accommodate the control rod guide tubes and small holes [5.08-cm (2-in.)

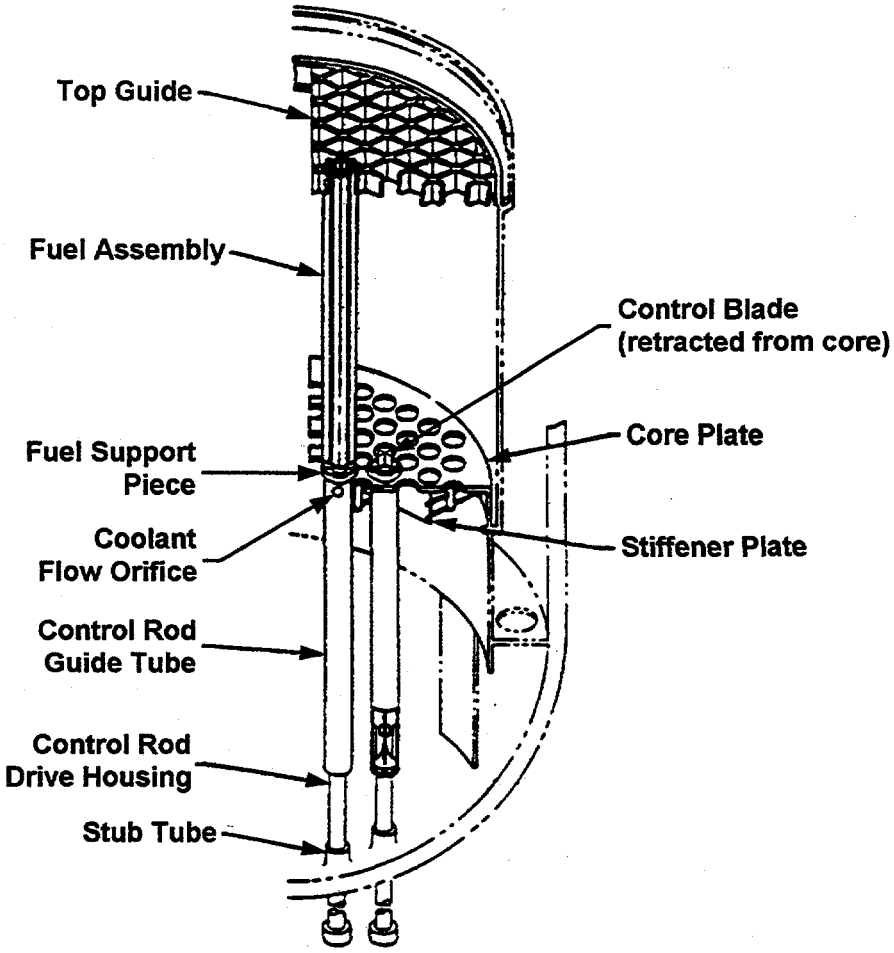

Figure 4. Position of core plate relative to other structures in BWR vessel.

diameter] for the instrument guide tubes. Vertical stiffener plates and perpendicular stiffener rods are located every 60.96 cm (24 in.) below the core plate to support the structure. The edge of the circular core plate assembly is bolted to a support ledge located between the lower shroud and the core shroud.

The other structures in the BWR core plate region illustrated in Figure 6 are also fabricated from stainless steel. The fuel support piece that sits on top of each control rod guide tube has four passages that direct coolant flow into the nose pieces at the bottoms of four fuel assemblies. There is also a cross-shaped opening in the center of each fuel support piece that allows the control blade to be inserted into and retracted from the core. During normal reactor operations, the control blades are fully retracted from the core as illustrated in Figure 4. After reactor scram during a severe accident, the control blades would be fully inserted into the core.

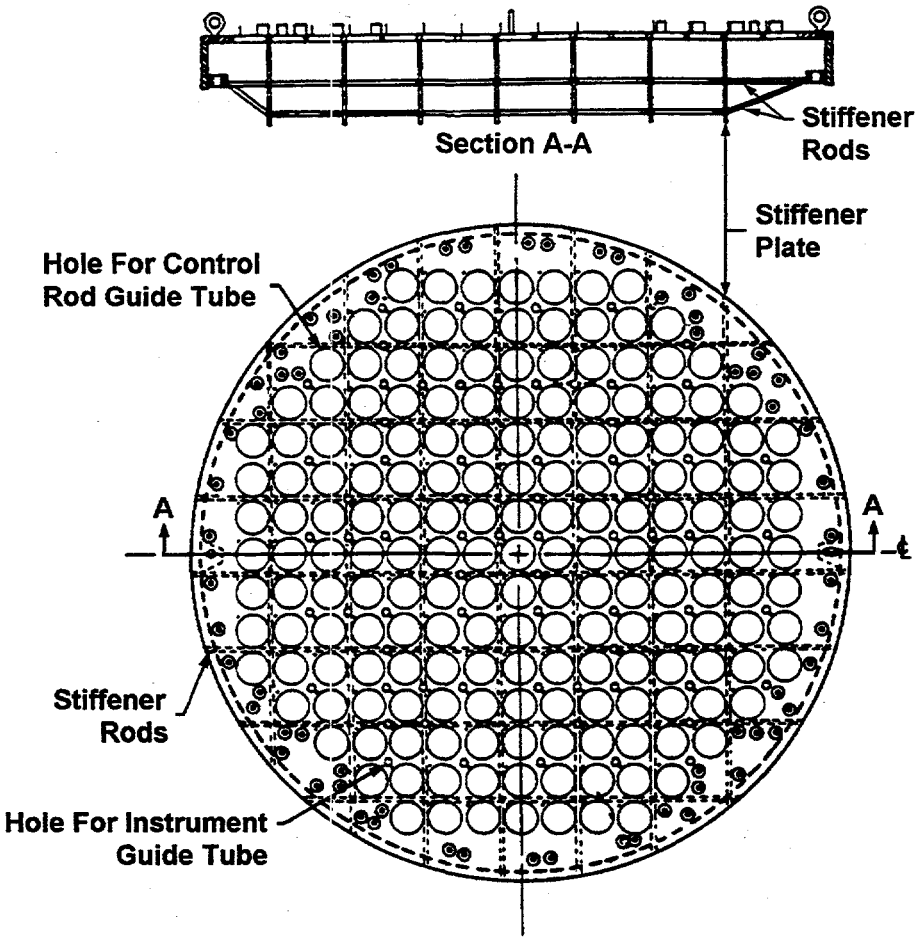

Figure 5. Top and side views of BWR core plate assembly.

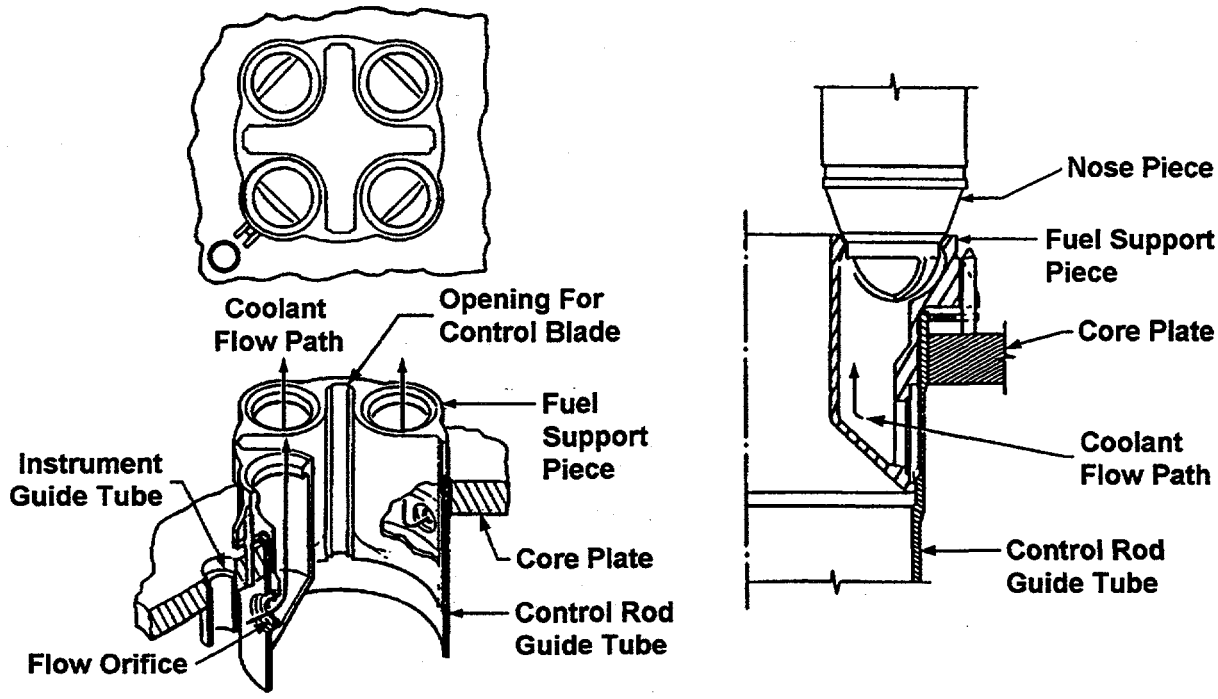

Figure 6. Detailed views of other structures located in BWR core plate region.

3. PHENOMENOLOGY

This chapter will characterize the relocation and degradation processes that are anticipated in the core plate region during a severe accident, by summarizing the results of several SCDAP/RELAP5 accident simulations for both PWR and BWR plants. Also, test results are presented for the XR2-1 experiment (conducted at Sandia National Laboratories), which is the only experimental information available for the response of the core plate region to a severe accident. These simulations and experimental results should provide an estimate of the range of conditions which a core plate model would be expected to handle, as well as an estimate of the amount and type of debris that is expected to relocate downward from the core into the core plate region.

3.1 Pressurized Water Reactor Processes

The history of SCDAP/RELAP5 application to PWR analyses is extensive. Most recently it has been used to characterize the probability of containment failure by direct containment heating (DCH), and those analyses will be used to characterize the conditions the core plate model will be required to represent during a typical analysis. The descriptions of the transients provided here are intended to summarize a series of lengthy and well-documented analyses. For additional detail, please refer to the appropriate reference.

3.1.1 Surry DCH Study

The Surry DCH study[8] was a best-estimate SCDAP/RELAP5 analysis of the Surry PWR during a TMLB' sequence without recovery and without operator actions. The analysis was designed to evaluate the behavior of the reactor coolant system (RCS) and the progression of core damage with seal leaks of 480 gpm per reactor coolant pump (RCP). The sequence of events for this analysis can be summarized as follows: The reactor scrammed and RCPs tripped due to the loss of AC power at TMLB' initiation (at 0 s). Seal leaks of 21 gpm per RCP were introduced at that time to simulate leakage associated with the loss of seal cooling that would accompany the loss of AC power. An initial RCS pressure reduction occurred because boiling on the SG secondary side was sufficient to remove core decay heat and cool the RCS. However, the steam generator (SG) heat sinks were not sustainable without feedwater, and the RCS pressure began to increase following SG dryout. The pressure increase terminated at the pressurizer PORV opening set point and a gradual RCS heatup and boiloff followed where PORV cycling provided pressure control between 15.8 and 16.3 MPa. When saturated conditions were reached at the RCPs, seal leaks were increased to 480 gpm per RCP to simulate failures that could develop with two-phase flow across the seal faces.

Core decay heat was transported to the SGs by full loop natural circulation of liquid until vapor generated in the core had collected in the top of the SG U-tubes, preventing further liquid circulation. Energy dissipated through RCP seal leaks exceeded core decay heat after 8980 s. As a result, the RCS pressure dropped below the PORV set point, which ended further PORV cycling. The first core uncovery began at 8783 s and was complete by 10 372 s as a result of boiling and venting through the RCP seals. By 8900 s, voiding in the SG tubes and hot legs allowed development of hot leg countercurrent natural circulation. Heat transfer to the ex-vessel piping by the countercurrent flow produced a heatup and an associated creep rupture failure of the hot leg in the pressurizer loop at 22 975 s. A 0.150 m diameter break was introduced at the time of hot leg failure, allowing further RCS pressure reduction and injection of the remaining accumulator inventory. The accumulators emptied at 23 200 s, with a core collapsed liquid level

~0.22 m below the top of the fuel rods. A second heatup and boiloff at low RCS pressure followed, with a second (and final) core uncovery completed at 24 056 s.

The first formation of an in-core molten pool occurred as a result of heating to ceramic melt conditions at 12 213 s. However, accumulator injections (starting at 12 362 s) delayed further melting until 27 649 s, when control rod absorber materials began to melt and relocate to the lower head. Core melting followed since accumulators (the only cooling water source) emptied by 23 200 s. The melt spread both axially and radially until the pool reached the core periphery at 32 406 s. At that time, the contents of the in-core molten pool (58 648 kg of UO2, 14 966 kg of ZrO2) was relocated to the lower head over a 60 s time period. Following the first core relocation to the lower head, a second relocation of molten materials (4976 kg of UO2 and 1170 kg of ZrO2) took place at 36 260 s. A summary of the lower head debris at the end of the simulation is provided in Table 2.

Table 2. Debris parameters during Surry DCH study.

Lower Head Debris Characterization	
Ag - In - Cd	*1,923 kg*
UO2	*63,624 kg*
ZrO2	*16,136 kg*
Maximum temperature	*3653 K*
Average molten temperature	*3303 K*
Molten Fraction	*0.70*

3.1.2 Zion DCH Study

The Zion DCH study[9] was a best-estimate SCDAP/RELAP5 analysis of the Zion PWR during TMLB' sequences without recovery and without operator actions. The Zion transient was designed to be very similar as the Surry transient just described, but three cases of varying RCP seal leak rates were considered. The range of debris values from all three cases are presented in Table 3.

The behavior of the Zion PWR was as follows: The reactor scrammed and RCPs tripped due to the loss of AC power at TMLB' initiation (at 0 s). Once again seal leaks of 21 gpm per RCP were introduced at that time to simulate leakage associated with the loss of seal cooling that would accompany the loss of AC power. An initial RCS pressure reduction occurred because boiling on the SG secondary side was sufficient to remove core decay heat and cool the RCS. However, the SG heat sinks were not sustainable without feedwater. As a result, the RCS pressure began to increase following SG dryout (at~4800-5000 s). The pressure increase terminated at the pressurizer PORV opening set point, which was reached at 5680 s A gradual RCS heatup and boiloff followed with PORV cycling providing pressure control between 15.7 and 16.2 MPa. Saturated conditions were reached at the RCPs at 7466 s. Seal leaks were increased to 480 gpm per RCP at that time to simulate failures that could develop with two-phase flow across the seal faces.

Core decay heat was transported to the SGs by full loop natural circulation of liquid until 7526 s. By that time, vapor generated in the core had collected in the top of the SG U-tubes, preventing further liquid circulation. Energy dissipated through RCP seal leaks exceeded core decay heat by 8456 s. As a result, the RCS pressure dropped below the PORV set point, which ended further PORV cycling. The pressure

reduction resulting from RCP seal leak flows persisted until the initial accumulator pressure of 4.24MPa (and the associated injection) was reached at 12 312 s. The first core uncovery began at 8644 s and was complete by 10 016 s as a result of boiling and venting through the RCP seals. By 8697 s, voiding in the SG tubes and hot legs allowed development of hot leg countercurrent natural circulation. Heat transfer to the ex-vessel piping by the countercurrent flow produced a heatup and an associated creep rupture failure of the hot leg in the pressurizer loop at 20 650 s. A 0.166 m diameter break was introduced at the time of hot leg failure, allowing further RCS pressure reduction and injection of the remaining accumulator inventory. The accumulators emptied at 20 920 s, with a core collapsed liquid level 0.82 m below the top of the fuel rods. A second heatup and boiloff at low RCS pressure followed, with a second (and final) core uncovery completed at 21 470 s.

The first formation of an in-core molten pool occurred as a result of heating to ceramic melt conditions at 12 169 s. However, accumulator injections (starting at 12 312 s) delayed further melting until 26 610 s, when control rod absorber materials began to melt and relocate to the lower head. Core melting followed since accumulators (the only cooling water source) emptied by 20 920 s. The melt spread both axially and radially until the pool reached the core periphery at 29 212 s. At that time, the contents of the in-core molten pool (60 290 kg of UO2 and 16 690 kg of ZrO2) was relocated to the lower head over a 60 s time period (Note that some debris had accumulated from prior relocations of control rod materials.)

Table 3. Debris parameters during Zion DCH study.

Core Plate Debris Characterization	Minimum	Maximum
Ag - In - Cd	*200(kg)*	*2350(kg)*
UO2	*61040(kg)*	*82550(kg)*
Zr	*0*	*452(kg)*
ZrO2	*15770(kg)*	*20860(kg)*
Maximum Temperature	*3775 K*	*4108 K*
Average molten temperature	*3415 K*	*3794 K*
Molten Fraction	*.81*	*1.0*

3.2 Boiling Water Reactor Processes

This section describes the damage progression that is expected to occur in the BWR core plate region during a severe accident. First, the results of a severe accident simulation for the Browns Ferry BWR design are presented to provide an estimate of the amount and type of debris that is anticipated to relocate downward from the core into the core plate region. Refer to Reference 10 for a description of the SCDAP/RELAP5 input deck for Browns Ferry and for a more complete presentation of the predicted results. Then, some test results are presented for the XR2-1 BWR metallic melt relocation experiment conducted at Sandia National Laboratory, which is the only experimental information available for the severe accident response of the core plate region.

3.2.1 Browns Ferry BWR Simulation Results

A SCDAP/RELAP5 calculation was performed for the Browns Ferry BWR design based upon a short-term station blackout (STSB) accident sequence.[10] This section includes only the calculated results that are relevant to the structures in the core plate region. The initial condition for the Browns Ferry STSB accident simulation is steady-state reactor operation at full power. The STSB accident sequence is caused by a loss of off-site AC power combined with failure of the emergency diesel generators and is initiated in the SCDAP/RELAP5 simulation by: (1) loss of AC power to the recirculation pumps and the CRD cooling water pumps, (2) main steam isolation valve (MSIV) closure, (3) reactor scram, and (4) loss of the turbine-driven feedwater pumps followed by feedwater coast-down. Throughout the duration of the STSB accident sequence, all sources of Emergency Core Cooling System (ECCS) injection are unavailable. The calculated results for the STSB accident simulation are summarized in the following discussion.

After reactor scram and MSIV closure at the beginning of the accident, steam continues to be generated within the vessel because of the decay power. This steam is released to the suppression pool by the safety/relief valves (SRVs) that open and close to maintain the vessel pressure between 6.516 MPa (945 psia) and 7.688 MPa (1115 psia). As steam is released from the vessel, the vessel water level falls and reaches the top of active fuel at 3,502 s after scram (see Table 4). When the water level reaches one-third of the active fuel height at 5,922 s, the reactor operators initiate the Automatic Depressurization System (ADS). The vessel water inventory flashes to steam during the depressurization, stabilizing in the lower

plenum at a level well below the core plate; thus the core and core plate regions are dry prior to the beginning of any structural degradation.

Table 4. Predicted event times for Browns Ferry STSB accident

Description of Event	Time After Scram (s)			
Short-term station blackout accident initiation	0			
Collapsed water level at top of active fuel	3,502			
ADS initiation (collapsed water level at one-third active fuel height)	5,922			
	Ring 4 (periphery)	Ring 3	Ring 2	Ring 1 (center)
First control blade liquefaction (1505 K)	10,068	8,340	8,004	7,740
First relocation of molten metallic material below bottom of active fuel	11,556	8,400	8,124	7,860
First blockages between control blades and channel boxes	11,763	8,643	8,388	7,992
First fuel cladding relocation (2200 K)	12,060	9,120	8,410	8,348
Molten ceramic pool (occupying 3 of 4 core radial rings) begins to relocate downward from core region into lower plenum	12,038			
Remaining water evaporates from lower plenum	13,692			
Creep rupture failure of bottom head	22,095			

After the core becomes uncovered, it begins to heat up. The radial power distribution is represented in the Browns Ferry simulation by dividing the core into four radial rings identified as Rings 1 (center of core) through 4 (periphery of core). Control blade liquefaction begins in Ring 1 at 7,740 s (refer to Table 4) when the control blades reach a temperature of 1505 K. The molten control blade material relocates downward and either solidifies at lower elevations in the core or falls below the bottom of active fuel (beginning in Ring 1 at 7,860 s). When sufficient freezing occurs, blockages form between the locally intact control blades and the outer surfaces of the channel boxes (beginning in Ring 1 at 7,992 s). The portion of the fuel cladding which has not oxidized begins to relocate in Ring 1 at 8,348 s when the cladding oxide layer fails at a user-specified temperature of 2200 K. The degradation processes are similar in Rings 2 through 4, except they occur at progressively later times because the decay power is smaller near the periphery of the core.

Some of the control blade/channel box material that initially solidifies in the lower core region melts again and also relocates downward below the bottom of active fuel. Because the current version of SCDAP/RELAP5 does not represent the severe accident response of the core plate region structures, this molten metallic material falls directly into the lower plenum to form a debris bed (represented by the COUPLE module) with the height shown in Figure 7. The molten metallic material falls below the bottom

of active fuel at a fairly steady rate for a 1,968-s period from 7,860 to 9,828 s after scram. At the end of this period, a total of 13,700 kg of metallic material has relocated from the core region, which is more than the total mass of the Browns Ferry core plate assembly (9,300 kg). Therefore, it is expected that the molten metallic material (at temperatures >1500 K) relocating below the bottom of active fuel should cause significant heating of the core plate and surrounding structures that is not currently represented in SCDAP/RELAP5 (these structures are currently represented by RELAP5 heat structures and their predicted temperatures never exceed 500 K).

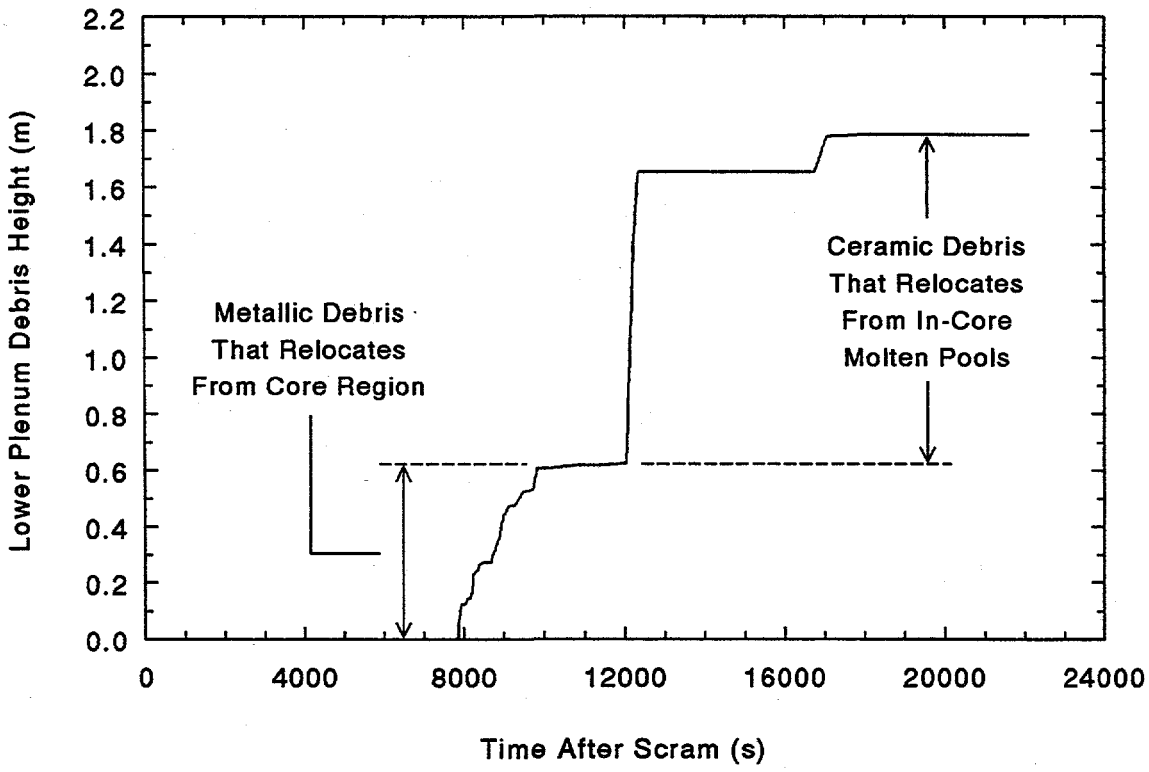

Figure 7. Predicted lower plenum debris height for Browns Ferry STSB accident.

As heating of the core continues, fuel rod degradation leads to formation of a large molten ceramic pool that occupies three of the four core radial rings. This molten pool is held in place by a frozen crust that can propagate both axially and radially into any surrounding porous debris. Spreading of the molten ceramic pool occurs when the heat flux from the molten pool to the inside surface of the crust is greater than the heat flux from the outside surface of the crust to the coolant. At 12,038 s, the in-core molten pool, which is at a temperature of 2934 K, is calculated to begin relocating downward into the lower plenum (this relocation process takes 300 s, refer to Figure 7). The printed output for the Browns Ferry STSB accident simulation indicates that the supporting crust fails in Ring 1 because the crust propagates downward past the bottom of active fuel. The current in-core molten pool model in SCDAP/RELAP5 does not account for the structures in the core plate region. During an actual severe accident, however, it is expected that the molten pool would continue to spread down towards the core plate and the stainless steel structures in the core plate region would quickly melt unless there is a large cooling ate at the outside surface of the crust supporting the molten pool.

A second molten ceramic pool forms in the core region and begins to relocate downward into the lower plenum at 16,747 s. At the end of the Browns Ferry STSB accident simulation (creep rupture failure of the bottom head occurs at 22,095 s), a total of 159,644 kg of debris has fallen into the lower plenum. This debris consists of 7,662 kg of control blade material, 17,859 kg of Zr, 6,825 kg of ZrO_2, and 127,298 kg of UO_2.

3.2.2 Results of the XR2-1 Experiment

The only experimental information available for the behavior of the core plate region structures during a severe accident is from the XR2-1 BWR metallic melt relocation experiment performed at Sandia during October 1995.[11] The purpose of that experiment was to investigate the damage progression and the material relocation processes in the lower portion of a dry BWR core during the early phase of a severe accident (such as an STSB accident). The term "early phase" is used to refer to the period of the accident when the metallic structures (both stainless steel and Zircaloy) are melting and relocating. The XR2-1 test did not address the "late phase" of a severe accident after the ceramic fuel pellets begin to melt.

The XR2-1 test assembly (see the cross-sectional view in Figure 8) employed full-scale, prototypical BWR components and simulated a region from 50 cm above the bottom of active fuel downward to 20 cm below the core plate. The test assembly included portions of (1) fuel rods with depleted UO_2 pellets, (2) channel boxes, (3) nose pieces, (4) control blades with velocity limiters, (5) fuel support pieces with coolant flow passages, (6) control rod guide tubes, and (7) the core plate. The test package was surrounded by 5.08 cm (2 in.) of ZrO_2 fiber insulation to minimize radial heat losses.

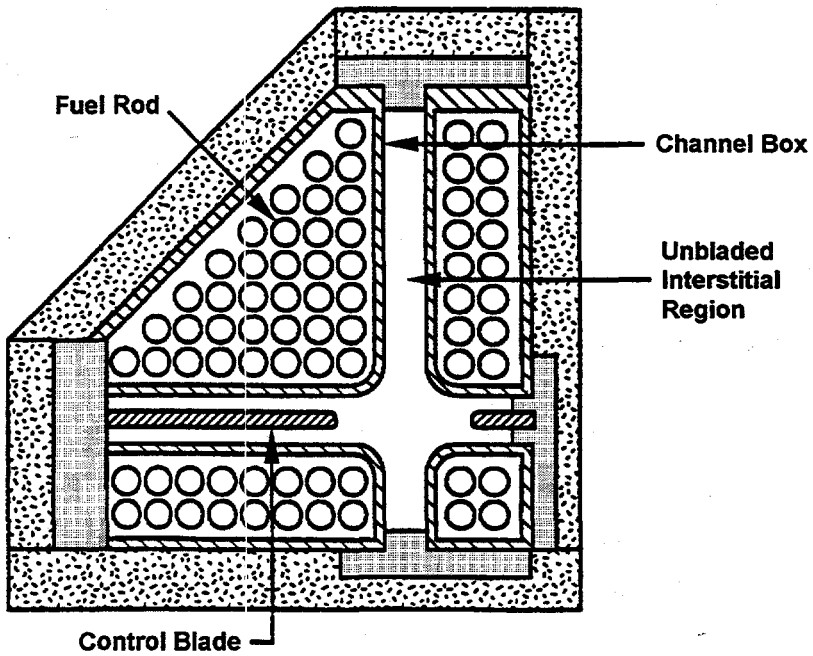

Figure 8. Cross-sectional view of XR2-1 test assembly

After preheating the XR2-1 test assembly to achieve a temperature gradient from about 1600 K (at the top of the assembly) to 580 K (at the core plate), molten metallic material was delivered into the top of the assembly using a wire feeding/melting system. First, 18 kg of a molten stainless steel/B_4C eutectic mixture was delivered at a steady rate during a 1,000-s period. Then, 35 kg of molten Zircaloy was delivered at a steady rate during a subsequent 950-s period. The stainless steel/B_4C feed points (10 total) were distributed above the control blades in the test assembly, and the Zircaloy feed points (31 total) were distributed above the fuel rods and the channel boxes.

The general behavior observed during the XR2-1 experiment was that the molten metallic material relocated downward and solidified when it flowed over cooler surfaces at lower elevations in the test assembly. After sufficient freezing occurred, localized blockages formed and caused additional molten material to pool on top of these blockages. As top-to-bottom heating of the test assembly continued, however, the blockages remelted, and the localized pools drained suddenly and flowed farther down into the test assembly. These sudden drainages caused some of the molten metallic material to bypass the core plate region completely and relocate downward past the bottom of the test assembly into a catch basin.

The Sandia staff identified three primary drainage paths as shown in Figure 9. The first drainage path was from the portion of the interstitial region where a control blade is inserted into the core, through the cross-shaped opening in the center of a fuel support piece (refer to Figure 6) and past the control blade velocity limiter inside a control rod guide tube. The second drainage path was from the unbladed portion of the interstitial region onto the top of the core plate. During the XR2-1 test, considerable inventory accumulated on the core plate, and some of that molten material flowed over the top of the fuel support pieces and contributed to the first drainage path. The third drainage path was from the fuel bundle region inside a channel box, through the nose piece at the bottom of a fuel assembly, and through the coolant flow passage of a fuel support piece (refer to Figure 6).

The Sandia staff determined that structural degradation in the upper half (i.e., the rodded region) of the XR2-1 test assembly was significantly accelerated by material interactions. First, the Zircaloy channel box walls were destroyed by aggressive eutectic reactions with the molten control blade material. Subsequently, when molten Zircaloy was being delivered into the top of the assembly, the upper half of the fuel rods were stripped of their cladding, and the fuel pellet stacks collapsed to form regions of porous debris.

Below the rodded region, the stainless steel structures retained their geometric integrity during the XR2-1 experiment. Although there were no outright failures of the nose pieces, fuel support pieces, or the core plate, about 75% of the total molten metallic inventory (53 kg of melted wire plus 9 kg of melted structures) relocated below the core plate through existing drainage paths. At the end of the test, this relocated material was located on top of the velocity limiters (~35% of total), inside the coolant flow passages at the bottom of the fuel support pieces (~10% of total), and in the catch basin below the test assembly (~30% of total). The balance of the molten metallic inventory (~25% of total) formed non-coherent localized blockages in the region on top of and just above the core plate. The molten material that drained into and through the core plate region heated the core plate from an initial value of 580 K to about 1150 K at the end of the test.

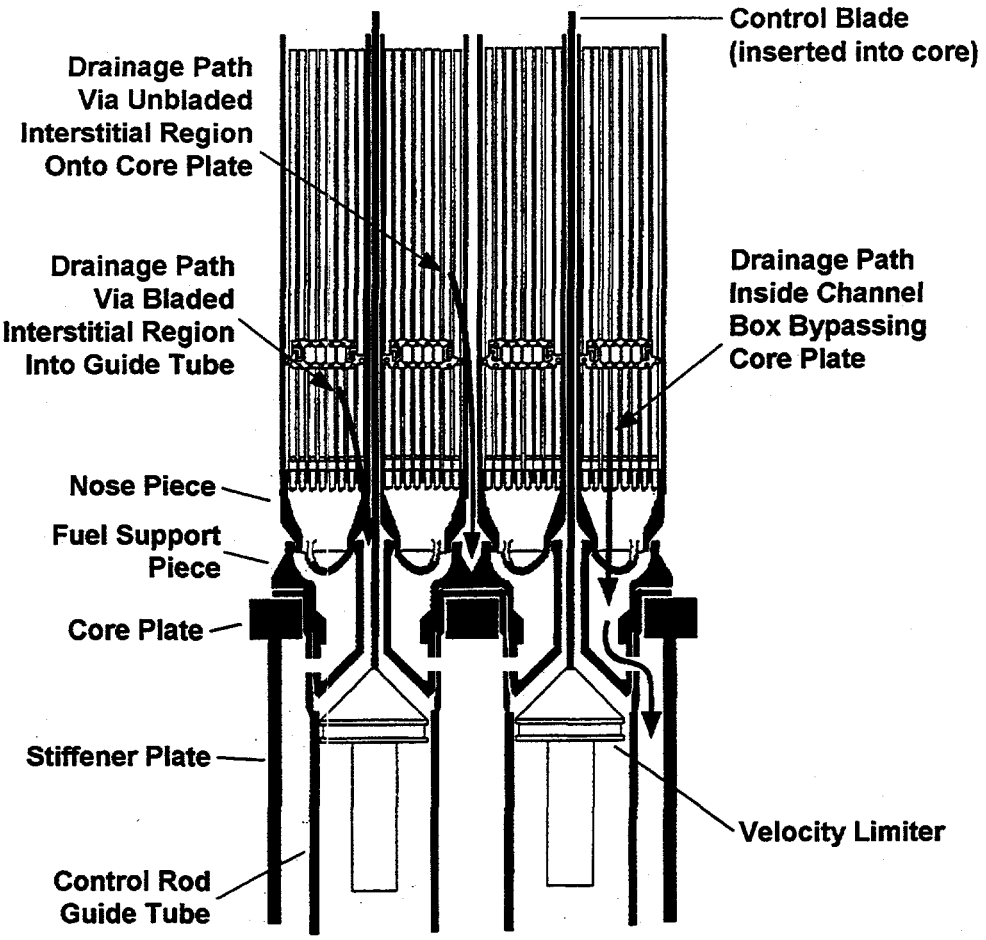

Figure 9. Drainage paths for molten metallic material during the XR2-1 experiment.

3.3 Summary of Debris Characterization

The experiment and analyses which have been summarized here indicate that relocation, whether from a PWR or BWR core, may occur in two stages. These stages are differentiated by the source and composition of the debris delivered to the lower core plate. The first stage consists of metallic debris and the second consists of a composite, primarily ceramic in nature, of UO_2, ZrO_2, and metals.

In the first stage, the control rods and other metallic structures within the core, melt, relocate, and refreeze in a lower/cooler region of the core. Then in a series of melt/relocate/refreeze cycles, these materials continue to move until they drop below the bottom of the active core. The debris state at the time it arrives at the core plate region is then a composite of primarily metallic materials, with a total mass on the order of 1-14 metric tons. This material is expected to be at approximately it's melting point, carrying little superheat, and will likely be completely molten. This material is expected to arrive at the core plate over a time span of thousands of seconds.

In the second stage, the core materials have melted and formed an in-core molten pool. This pool then gradually moves through the core region, both radially and axially, until it reaches either the periphery of the core or the bottom of the active core. At that time, the crust of the molten pool will fail and the

molten contents of the pool will relocate to the core plate region over a relatively short time frame. This material will consist of a composite of UO_2, ZrO_2, and metals, and may have a total mass in the range from of 80 to 130 metric tons. The material will be non-homogeneous, and may only be 70% molten, with entrained solids. The average molten material temperatures will be close to the melting temperature of UO_2, although highly localized regions may be as high as 3900-4000 K.

4. CORE PLATE MODEL DESCRIPTION

One of the goals for developing a core plate structure model has been to maximize the use of existing models within SCDAP/RELAP5. Based upon discussions between the NRC Technical Monitor, the SCDAP development staff at INEEL, and the BWR model development staff at ORNL, several modeling options have been identified: (1) utilize the existing lower plenum debris model (COUPLE module), (2) modify the existing upper plenum structure model, or (3) develop a completely new core plate structure model. Development of a new model was quickly eliminated because it was judged to be too costly.

In a typical SCDAP/RELAP5 simulation, the COUPLE module is utilized to represent the hemispherical region of the bottom head and any lower plenum debris. The user defines a two-dimensional finite-element mesh using cylindrical coordinates (radius and elevation). Each element in the mesh can be specified as either a solid material (e.g., carbon steel for the bottom head) or debris (initially filled with water). In theory, a single COUPLE mesh could be defined that extends from the bottom head upward to the bottom of the active core, including the core plate region. After extensive discussions, it was concluded that, although this method could provide a satisfactory representation of the thermal response of the core plate, the resources necessary to model the potentially intricate geometry and the damage progression expected to occur in the core plate region would also be too costly.

The upper plenum structure model in SCDAP/RELAP5 (see Appendix A) has many of the features needed for representation of the core plate region. This model includes calculations for heating (by convective heat transfer from the coolant), oxidation, melting, downward relocation, and solidification of pure stainless steel structures. The upper plenum structure model is based upon a slab geometry with rectangular coordinates and provides the user with sufficient flexibility to allow representation of a wide range of geometric configurations. Although the core plate region structures described in Chapter 2 are relatively complex, a slab geometry can be used to represent their thermal masses and heat transfer characteristics by using equivalent dimensions. This approach is judged to be the most economical way for modeling the damage progression that is expected to occur in the core plate region. The proposed model will represent the core plate region structures during the early phase of a severe accident through the time of metallic melting and relocation. Modifications to the core debris and molten pool models will also be required to represent the core plate region during the late phase of a severe accident.

4.1 General Approach

The approach used in the core plate model will be as follows:

The existing mass transfer of molten material from core region to lower head will be redirected to first deliver the material to the core plate model. Material which relocates beyond the boundary of the core region will be allowed to free-fall to the core plate, where it will be assumed to have zero velocity and momentum. The code user will have the capability of defining a flow path, expected to be along the core periphery, which will bypass the core plate model.

The structure of the core plate region will be represented with a combination of horizontal and vertical plates, similar to the current upper plenum structure model as described in Appendix A. The horizontal plates may have holes in them. There should be the capability of partitioning the area of the core plate model to represent those sections of the plate which are under one or more annular core rings.

Material which rests on the horizontal surfaces will interact thermally with the core plate. Molten material will have the possibility of forming a crust on the plate if sufficient cooling occurs. There will be self-leveling of molten material over the region which lies under one of the core annular rings, and no transfer of material from one annular ring to another until a threshold height is exceeded. No mechanical failure of the plate will be considered.

Molten material which lies over a core plate penetration will begin to relocate downward. If the material is metallic, a crust may form on the walls of the penetration and will have the capability of thickening until the penetration is blocked. If the material is primarily ceramic, no crust will form, but a slurry of two phase material will penetrate the core plate, until blockage is predicted to occur. In the event the material is predicted to relocate past the core plate, it will be passed to the fuel-coolant interaction (FCI) model.

4.2 Input

It will be necessary to add an additional subroutine, named 'rplate', which will process the additional input required for the core plate model. This additional input will consist of:

- A description of the specific core plate structure applicable to this analysis. This will consist of the number of structures, the number of axial levels to be modeled, the surface area and thickness of each structure, and the flow area through the structure.
- A description of the linkage between the core plate model and the remainder of the input model. This will consist of the number of radial core rings, and identify which portion of the core plate lies beneath each radial core ring, the hydrodynamic volumes in which the core plate structures reside, and linkages to the proper COUPLE mesh.
- Parameters to over-ride default values for heat transfer correlation, debris thickness to trigger spreading of molten material, plugging criteria, etc .

4.3 Modifications for Early Phase Phenomena

As currently modeled, molten material that drains downward from the core is either ignored, or , if a COUPLE mesh has been defined, falls directly into the lower plenum. This interface logic will be modified to redirect the flow of molten material, either from the core structures or from user-defined slumping to the core plate model, as shown in Figure 10. Material which drains below the core plate region will then either fall directly into the lower plenum, or be tracked by the Fuel-Coolant Interaction model, as appropriate.

The mass balance for the existing upper plenum structure model includes only stainless steel (74% Fe, 18% Cr, and 8% Ni) and its oxides. The mass balance for the core plate model must be expanded to include other materials that could drain from the core. These additional materials could include Zr, ZrO_2, dissolved UO_2, and neutron absorber materials such as B_4C or Ag/In/Cd alloy. Since the upper plenum model does not account for the effects of material interactions, the model must be modified to include the effects of material interactions because of the other materials (such as Zircaloy and neutron absorbers) that will drain downward from the core. It is recommended that melting and solidification of eutectic mixtures of stainless steel and other materials be represented in the core plate region energy balance by using reduced liquefaction temperatures in a manner similar to the BWR control blade/channel box model.

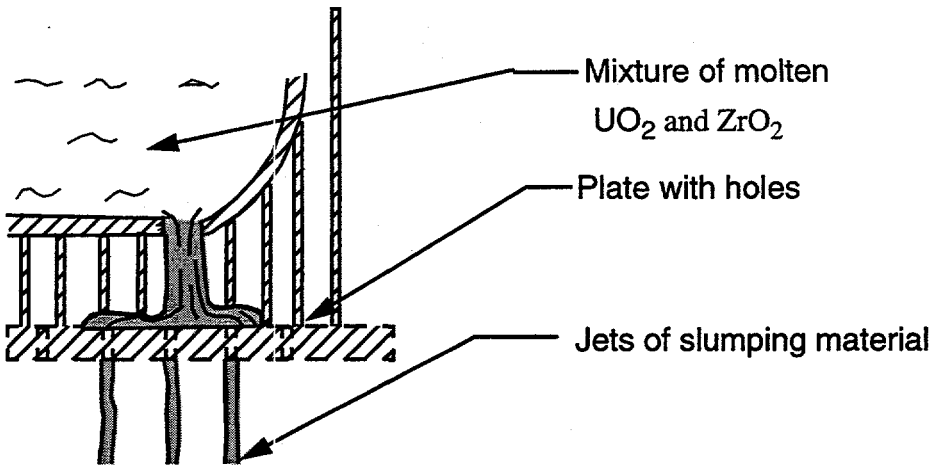

Figure 10. Representation of molten pool failure and material relocating to core plate.

Whenever other materials are present on the surface of a stainless steel structure in the core plate region, then a eutectic liquefaction temperature that is lower than the melting temperature of pure stainless steel will be used in the melting and solidification calculations.

If sufficient detail is specified by the user, there will be the capability of specifying a portion of the core plate model modeled as being directly below and connected to, each of several annular rings in the core. Within an annular ring the debris material will be represented with a uniform height (i.e., self-leveling) across the horizontal surface. Mass transfer to an adjacent annular ring will occur, either when the volume associated with the core plate is filled with debris, or alternatively when the debris height reaches a user-defined value. Once mass transfer is initiated, it will persist as long as the transfer criteria continues to be exceeded.

The core plate model will have the capability of tracking the formation of a crust of solidified material between molten debris material and the core plate. The heat flux on the inner surface of the crust that contacts the molten pool[a] is calculated using correlations developed from experimental data[12]. These correlations were developed from the results of experiments that measured the natural convection heat transfer coefficients at the boundary of a pool of fluid with internal heat generation and transient natural circulation. The heat flux at the lower boundary of the pool are calculated by the equation

$$q_b = 0.54 Ra^{0.18} \left(\frac{H}{R}\right)^{0.26} \frac{k\Delta T}{R} \qquad (1)$$

where

q_b = heat flux from molten pool to crust at bottom of molten pool (W/m^2)

Ra = Rayleigh number of the liquid in the molten pool

= $g\beta q_d L^5/\alpha\nu k$

a. The heat flux from the molten pool is calculated in identical manner to that for the in-core molten pool, as documented in Volume II of Reference 1.

k	=	thermal conductivity of the liquid in the molten pool (W/m•K)
ΔT	=	difference in temperature between temperature of molten pool and its melting temperature (K)
R	=	radius of molten pool at its upper surface (m)
H	=	depth of molten pool (m)
L	=	characteristic length (m) (assumed equal to depth of molten pool)
g	=	acceleration due to gravity (m/s^2)
β	=	volumetric coefficient of expansion (1/K)
α	=	thermal diffusivity (m^2/s)
ν	=	kinematic viscosity (m^2/s)
q_d	=	volumetric heat generation rate (W/m^3).

In the selection of transient natural convection, the heat flux at the lower boundary of the pool is calculated by the equation[13]

$$q_b = 0.472\left(\frac{H}{R}\right)^{0.317} Ra'^{0.220} k\frac{\Delta T}{R} \qquad (2)$$

where

Ra' = transient Raleigh number

$$= \frac{g\beta L^3 \Delta T}{\alpha\nu}.$$

Because of the continual addition of molten material to the upper surface of the pool, and minimal impact on results, the model will assume that no crust will form on the other surfaces of the molten pool.

4.4 Core Plate Blockage

The heart of the core plate model will be the modeling of blockage of the penetrations through the core plate. Without this blockage, no delay will occur in the arrival of the molten material to the lower head.

4.4.1 Metallic blockage

The upper plenum structure model allows for possible freezing of molten material on the surfaces of a structure, but does not include calculations to determine if the solidified material will form blockages that inhibit the downward movement of subsequent molten material. The justification for possible metallic blockage of the core plate is that the XR2-1 experiment (refer to Section 3.2.2) indicates that, at least for BWR geometries, molten material will relocate downward into the core plate region, solidify to form localized (non-coherent blockages, and then remelt in response to continued heating of the structures.

The flow of molten metallic material through the core plate penetrations will be limited by the formation of a layer of refrozen material along the sides of the penetration, as shown in Figure 11. The

formation of this layer will be modeled by tracking the formation of a crust on the surface of a vertical surface. As crust thickness increases, the flow area will be reduced until complete blockage of the core plate occurs. As additional molten material arrives at the surface of the core plate, increasing the temperature of the over-lying pool, melting of the crust may occur, with an appropriate increase in the flow area through the core plate.

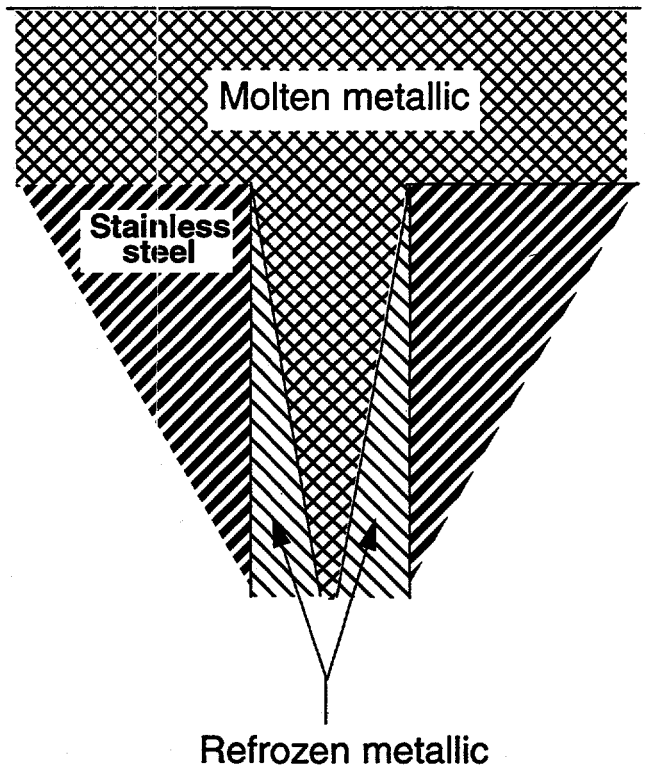

Figure 11. Blockage of core plate penetrations by metallic material.

4.4.2 Ceramic blockage

The available information about damage progression in the core plate region during the late phase of a severe accident (when the ceramic material forms an in-core porous debris bed and molten pool) is less definitive. The XR2-1 experiment did not address the late phase, but recent BWR and PWR accident simulations (See "PHENOMENOLOGY" on page 9.) predict that a large molten ceramic pool will propagate, either downward past the bottom of active fuel or peripherally to the core barrel and then downward into the core plate region. The core plate model must then determine whether this molten ceramic material quickly flows through the core plate penetrations, or whether the penetrations are plugged, thereby forcing the molten ceramic to melt through the core plate.

The results of experiments on UO_2 fuel flow and freezing are not consistent with the typical concept of molten material freezing on the sides of the penetration until sufficient crust growth plugs the penetration, as described in the previous section. A conduction controlled analytical formulation for solidification predicts that molten material penetrates significantly greater distances before plugging occurs than is experimentally observed[15]. It has been concluded that UO_2 flowing over steel behaves in a

manner that prevents the formation of a stable crust at the the wall and, therefore, UO_2 penetration is controlled by turbulent heat transport from the slug of molten ceramic material to the structure. This conclusion leads to the concept of the material flow illustrated in Figure 12, which shows the existence of a two-phase ceramic slurry flowing through the core plate penetration with no crust formation along the walls. In such a case, the plugging of the core plate penetrations can not be modeled using the traditional methods described for the metallic plugging.

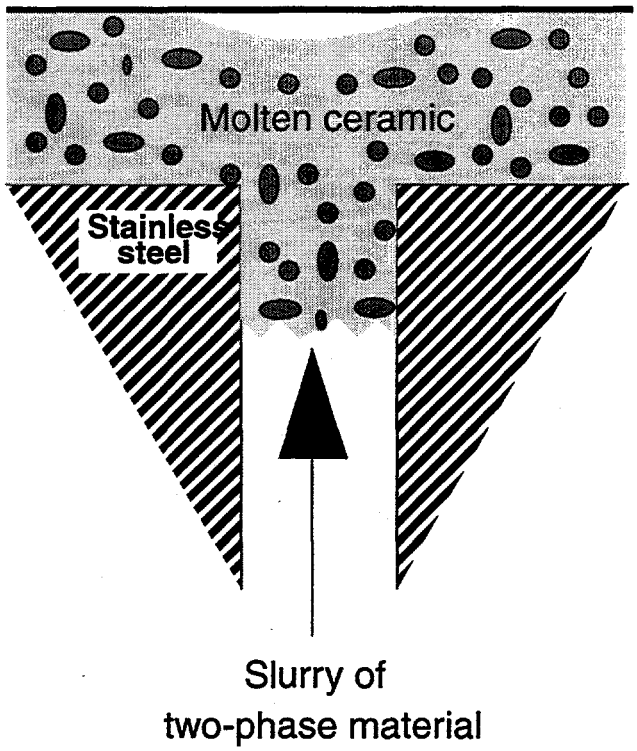

Figure 12. Blockage of core plate penetration by ceramic material.

In order to model the plugging of the core plate penetrations by molten ceramic material, a correlation for the penetration of a flowing ceramic through a steel channel[14] will be used. If the correlation predicts that the slurry will penetrate a distance less than the core plate thickness, then the penetration will be modeled as plugged. This correlation for the core plate penetration distance is:

$$X_P = \frac{1}{2}\frac{D}{f}\left(\frac{\frac{L_f}{c_f} + T_{f,0} - T_{f,mp}}{T_{f,0} - T_{s,mp}}\right)\left(\frac{1}{1 + \frac{T_{f,mp} - T_{s,mp}}{\frac{L_s}{c_s} + T_{s,mp} - T_{s,0}}}\right) \quad (3)$$

where

X_p = Penetration distance

D = channel diameter

f = coefficient of friction
L = latent heat of fusion
c = heat capacity
T = Temperature (subscripts f = fuel, s = steel, mp = melting point, 0 = temperature at channel entrance or initial wall temperature.

4.5 Core Plate Failure

Although there is no significant evidence to suggest that a lower core plate will experience failure, it does seem reasonable to allow the possibility that, if blocked, the core plate will fail. Additionally this will provide some upper bound on the period of time that the arrival of molten material in the lower head will be delayed.

4.5.1 Thermal failure of core plate

Thermal failure of the core plate will be modeled by using existing capability within the upper plenum structure model. Heat is transferred into the core plate using the correlation described in Section 4.3 and tracked using the heat conduction solution described in Appendix A. Melting of the core plate under the crust will be tracked in a separate variable and when the melt front approaches the lower surface of the core plate, the plate will be modeled as failed.

A question about the survivability of the crust between a pool of molten ceramic material and the stainless steel core plate remains unresolved, particularly after the discussion of Section 4.4.2, which states that the crust does not survive but rather is swept into the molten pool. Intuitively, it would appear obvious that even at the solidus temperature of a U/Zr/O mixture, a sufficient mass of the substrate stainless steel would be molten to cause the crust to "float" between two liquid layers, and that such a situation would not routinely lead to a stable crust. If the crust is indeed unstable, then the thermal attack of the molten ceramic pool upon the stainless steel core plate is not limited by conduction through the crust, and the solid surface is immediately exposed to the molten pool bulk temperature. Under the handicap of a lack of experimental evidence either way, the SCDAP/RELAP5 core plate model will have an input switch allowing the user to control the survivability of the crust. It is recommended that during the testing of the core plate model, this switch be exercised to evaluate it's impact on the resulting transient.

4.5.2 Structural failure of core plate

There is considerable uncertainty concerning the possible structural failure mechanisms of a core plate. Although the PWR's described in Section 2 utilize structures within the core plate region to support reactor vessel internals, it is beyond the scope of SCDAP/RELAP5, either to demand that the code user specify reactor vessel internal structure, or if specified, to perform a detailed structural analysis.

In a BWR, where the weight of the core is supported by the bottom head via the control rod guide tubes, there is initially very little physical load on the core plate (i.e., the core plate assembly must support only its own weight). As molten metallic material drains or porous ceramic debris settles onto a BWR core plate, the loading can increase. However, the presence of solidified metallic material on top of the core plate will most likely cause the core plate to become partially "welded" to the top of the control rod guide tubes. Thus, much of the debris load on a BWR core plate could also be supported by the bottom head

rather than the outer edge of the core plate assembly. If a BWR core plate does not become "welded" to the top of the control rod guide tubes, then two modes of structural failure are possible in response to the combined thermal and physical loads. Localized failures of the core plate could occur between the vertical stiffener plates that are positioned every 60.96 cm (24 in.) below the core plate (refer to Figure 5). A core-wide failure of the entire core plate assembly is also possible.

Because of the uncertainties in core plate failure mechanisms, and also because the XR2-1 experiment indicates that a BWR core plate should remain intact during the early phase of a severe accident, it is recommended that the core plate model not include any structural failure calculations.

4.6 Future Work

The authors have discussed phenomena which due to limited resources have not been included in the existing design, but which could be added in future, if the application of the model shows that additional detail is justifiable. These potential extensions consist of:

- radiation heat transfer between core region and core plate region,
- refinement of assumption of self-leveling across a single core plate region,
- refinement of assumption regarding radial movement of molten material upon the core plate, and
- calculation of stress failure of core plate.

The most significant deficiency in the existing core plate design is the lack of radiation heat transfer between core region and core plate. The authors have not included this phenomena in the design because it was our judgement that accident scenarios which have removed sufficient structure between core and core plate to allow significant radiation heat transfer will also leave a puddle of molten material on the upper surface of the core plate. This molten material will be at sufficiently high temperatures to minimize radiation heat transfer. Additionally, adding the capability of modeling radiation heat transfer would significantly increase the input burden placed upon the code user to adequately describe the geometry of the region between core and core plate. It is therefore our recommendation that radiation heat transfer between core and core plate be ignored until application of the core plate model to reactor safety analyses demonstrates the need for additional capability.

The movement of molten material upon the upper surface of a core plate has been minimized in the current design. Assumptions regarding self-leveling across a single core plate region, and radial relocation between regions seem adequate for the specified design goals of the core plate model. However, if reactor safety applications demonstrate the need for a more mechanistic model, it should be possible to extend the model to more adequately model flow acros the plate.

The extension of the core plate model to include a structural failure calculation as well as the existing thermal failure seems to be inconsistent with a design objective of estimating arrival of molten material to the lower head. It is the authors judgement that the additional complexity of such a model would add little to the answers provided by the model. Once again, however, if applications should the need, such a model could be added.

5. TESTING

Validation of the core plate model will be done by performing the following three tests.

5.1 Simple Cheap Vessel Problem

The Simple Cheap Vessel Problem (SCVP) is a benchmark problem sent with each code transmittal, which is fast running but tests the heatup of core components and the relocation of core material into the lower head. The hydrodynamic model consists of two parallel flow channels with time-dependent volumes at each end to set flow conditions, as shown in Figure 13. Each flow channel has a fuel rod component, representing 18,408 fuel rods, and a control rod component representing 118 Ag/In/Cd control rods. These core components are connected to a COUPLE mesh representing the lower vessel head.

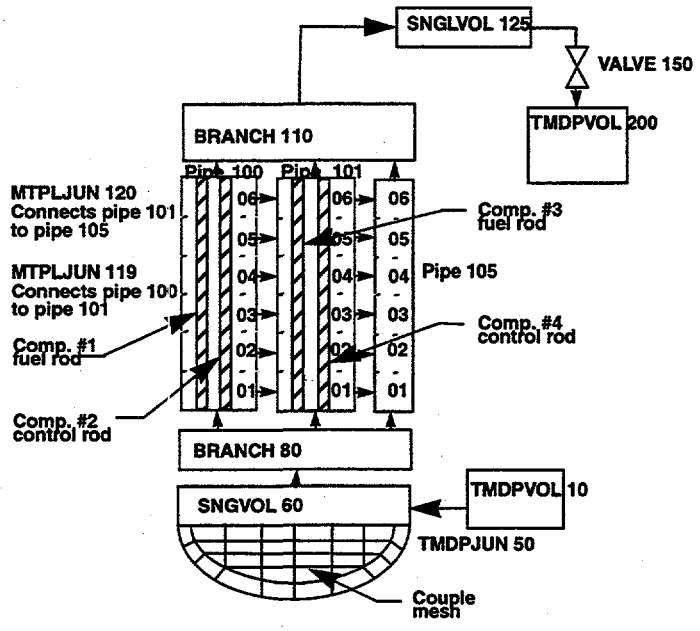

Figure 13. Nodalization of Simple Cheap Vessel Problem

The simulation is conducted under conditions which are intended, not to provide prototypical response, but instead to drive the simulation into core melting and relocation in an accelerated manner. The simulation is therefore initiated with the fuel rods at the following conditions:

- a uniform temperature of 900 K,
- a constant core power of 934 MW, and
- a saturated steam environment.

The primary purpose of the simulation will be to test the interface logic between the core relocation module, the lower core plate module, and the lower head module. The simulation will also be used to test the thermal response of the core plate, and the radial relocation of materials upon the core plate.

5.2 User-Defined Slumping Problem

As described in the previous section, the model will have the capability of taking a description of molten material slumping onto the plate, not from the SCDAP/RELAP5 core models, but from user input. The advantage of this capability is that anyone, who wishes to verify the model, may define slumping characteristics which may examine only the metallic relocation aspects of the model, for instance. Such a set of conditions might be difficult or time-consuming to establish using only the existing core models.

The user-defined slumping problem will simulate a core plate of three annular sections of equal surface area, as shown in Figure 14. Three possible sources of slumping will be defined, one for each annular ring. A variety of slumping rates, temperatures, and compositions will be established to exercise specific aspects of the core plate model. Because of the wide variety of conditions that may be specified, as well as the specificity of the slumping characteristics, this problem is intended to provide the primary tool for examing the validity of the core plate model capabilities.

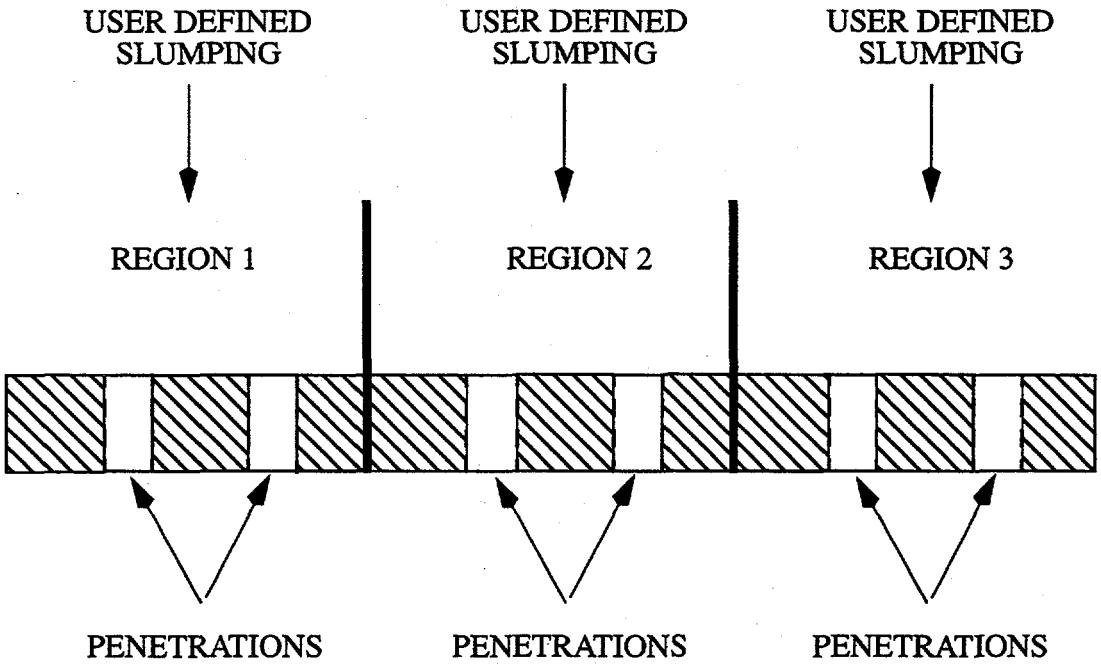

Figure 14. User defined slumping problem geometry.

The user-defined slumping problem will be used to examine the models capability to:

- handle material compositions typical of both PWR and BWR safety analyses,
- model core plate thermal response,
- model both metallic and ceramic penetration of the core plate, and
- model radial relocation of molten material on the upper surface of the core plate.

5.3 XR2-1 Experiment

Any model designed to be applied to the core plate region would obviously be expected to be assessed against an experiment designed to investigate the material relocation processes and pathways

during a severe accident, such as the XR2-1 experiment. The availability of experimental data in a phenomenological region such as this is a resource which can not be ignored. However, as is often the case when an analysis examines complex processes which are competing for effect, the effort to impose the proper boundary conditions and to model the most significant phenomena, can exceed the resources available for a task such as this. Even the report which documents this experiment[11] concluded that MERIS, the stand-alone code used in the post-test analysis, was unable to predict much of the relocation phenomena encountered during the experiment, despite extensive modifications to model non-prototypic boundary conditions.

The authors therefore recommend that the assessment of the SCDAP/RELAP5 core plate model focus on the phenomenology of the XR2-1 experiment, rather than a detailed assessment of the experiment itself. This phenomenology, described in Section 3.2.2 and repeated in Figure 15, can be modeled with the user-defined slumping capability as described for the previous assessment case..

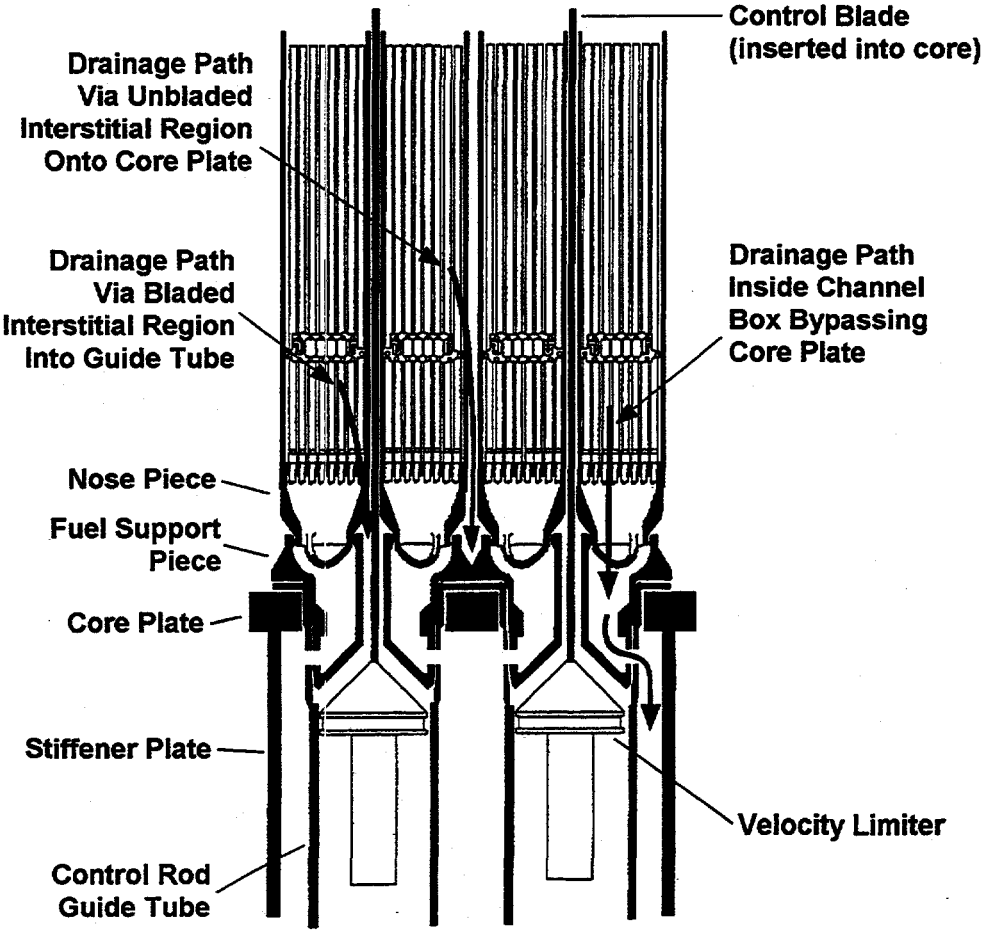

Figure 15. XR2-1 drainage flow paths.

6. CONCLUSIONS

This report has described a design to extend SCDAP/RELAP5 to model the core plate region of either a PWR or BWR plant. Such a model is necessary because experimental evidence, as well as several analyses, have indicated that metric tons of molten core material can relocate into and through the core plate region. If oxidation in the core is limited by the availability of steam, and if the lower head still contains coolant, then the relative timing of the arrival of molten core material into that coolant can be significant to the course of the accident analysis. SCDAP/RELAP5 currently assumes that molten material which leaves the core region falls into the lower vessel head with no delay due to interaction with structural materials. The objective of this design report is to describe the modifications required to treat the thermal response of the structures in the core plate region as molten material relocates downward from the core, through the core plate region, and into the lower plenum.

A survey has been performed to characterize the structures in the core plate regions of both PWR and BWR designs. Additionally, a survey of available experimental data and several recent analyses for both PWR and BWR plants was performed to characterize the range of conditions which a core plate model could be expected to experience. The survey of geometries showed that a wide variety of core plate geometries must be modeled, with thicknesses varying from 5 to 55 cm. The data survey demonstrated that relocation, whether from a PWR or BWR core, may occur in two stages. The first stage consists of metallic debris with a total mass on the order of 1-14 metric tons, and approximately at it's melting point. The second consists of a composite, primarily ceramic in nature, of UO_2, ZrO_2, and metals, and may have a total mass in the range from of 80 to 130 metric tons. The material will be non-homogeneous, and may only be 70% molten, with entrained solids. The average molten material temperatures will be close to the melting temperature of UO_2, although highly localized regions may be as high as 3900-4000 K.

A model has been described which will allow SCDAP/RELAP5 to track the behavior of molten material as it passes through the core plate region, with particular emphasis on estimating the relative time of the arrival of that molten material to the lower vessel head. The model will make use of the existing upper plenum structure model, to model the thermal response of the plates, with additional modeling to model the retention of that material on the core plate. In addition, a series of tests have been described which will verify the model over the range of conditions described.

7. REFERENCES

1 C. M. Allison, et al., SCDAP/RELAP5/MOD 3.2 Code Manual, NUREG/CR-6150 Rev. 1, Idaho National Engineering and Environmental Laboratory, October 1997.

2 C.M. Allison and S.A. Chavez, *Proposed SCDAP/RELAP5/MOD3.1 Model Additions to Treat the Behavior of Upper Plenum and Core Plate Structures During the Later Phases of a Severe Accident (Draft)*, EGG-RAAM-11500, September 1994.

3 *Final Safety Analysis Report, Three Mile Island Unit 2*, Metropolitan Edison Company.

4 *Final Safety Analysis Report, Waterford Steam Electric Station Unit 3*, Energy Operations Incorporated.

5 *Final Safety Analysis Report, Calvert Cliffs Units 1 and 2*, Baltimore Gas and Electric Company.

6 *Final Safety Analysis Report, Braidwood Nuclear Power Plant Unit 1*, Commonwealth Edison Company.

7 *Final Safety Analysis Report, Zion Station*, Commonwealth Edison Company.

8 M.M. Pilch, et al., *The Probability of Containment Failure by Direct Containment Heating in Surry*, Appendix E, NUREG/CR-6109, May 1995.

9 M.M. Pilch, et al., *The Probability of Containment Failure by Direct Containment Heating in Zion*, Appendix C, NUREG/CR-6075 Supp. 1, December 1994.

10 F. P. Griffin, *SCDAP/RELAP5 Mod 3.2 Simulations For the Browns Ferry BWR Design*, ORNL/NRC/LTR-97/27, letter report to Dr. Y. Chen, Accident Evaluation Branch, Division of Systems Technology, RES, NRC, December 16, 1997.

11 R. O. Gauntt and L. L. Humphries, *Final Results of the XR2-1 BWR Metallic Melt Relocation Experiment*, NUREG/CR-6527, SAND97-1039, Sandia National Laboratories, August 1997.

12 M. Jahn and H. H. Reineke, "Free Convection Heat Transfer with Internal Heat Source, Calculations and Measurements," *Proceedings of the International Meeting on Thermal Nuclear Reactor Safety*, NUREG/CR-0027, 2, February 1983, pp. 996-1010.

13 C. M. Allison, J. L. Rempe, and S. A. Chavez, *Final Design Report on SCDAP/RELAP5 Model Improvements - Debris Bed and Molten Pool Behavior*, INEL-96/0487, December 1996.

14 M. Epstein, et al., "Transient Freezing of a Flowing Ceramic Fuel in a Steel Channel", *Nuclear Science and Engineering*: 61, 310-323 (1976).

15 D.H. Cho, M. Epstein, R.P. Anderson, D.R. Armstron, "Transient Freezing in a Tube Flow," in Reactor Development Program Progress Report, ANL-RDP-37, 7.12, Argonne National Laboratory (1975).

APPENDIX A. UPPER PLENUM STRUCTURE MODEL

The upper plenum structure (UPS) model for SCDAP/RELAP5 has been developed to represent the severe accident response of structures located in the upper plenums of PWRs or BWRs. It includes generalized features that allow a single model to represent a range of geometric configurations. Unlike the RELAP5 heat structure model, the UPS model includes calculations for oxidation, melting, and downward relocation. This appendix provides a brief description of the model used to represent the upper plenum structures.

A1 Nodal Geometry

The UPS model is based on the general configuration shown in Figure A-1. The user divides an upper plenum structure into axial levels (the example in Figure A-1 shows four axial levels). At each axial level, the structure can be defined as having either a vertical orientation (with left and right surfaces) or a horizontal orientation (with bottom and top surfaces). The temperature gradient through the structure is represented at each axial level by one or more conduction nodes defined by the user. Conduction and other heat transfer processes are modeled in a direction perpendicular to the structure orientation. Conduction heat transfer between axial levels is not considered.

The UPS model is based on a slab geometry with rectangular coordinates, but can be applied to a cylindrical structure such as a tube if the wall thickness is small relative to the radius of curvature. The physical dimensions specified by the user at each axial level are the structure surface area and the thicknesses of the conduction nodes. An upper plenum structure interacts with RELAP5 hydraulic volumes at both the left and right (or bottom and top) surfaces of the structure. This interaction includes convective heat transfer and oxidation.

All major structures in PWR and BWR upper plenums are made of stainless steel. The UPS model is therefore solved based upon the premise that there is a single material (stainless steel) with a unique melting temperature (i.e., there are no material interactions). Because the upper plenum structures have no internal heat sources, all heating and melting occurs at the outer surfaces. As a structure melts, molten material should not become superheated to any significant extent because either (1) the molten material will quickly relocate to a lower elevation or below the bottom of the structure or (2) more of the underlying solid structure will melt (this applies even when molten material accumulates on top of a horizontal surface).

A2 Energy/Conduction Equation With Melting

The differential equation for 1-D conduction heat transfer with melting is non-linear and requires a specialized solution method to account for the heat of fusion. A two-step process is applied in the UPS model. First, the conduction equation is solved without consideration of melting using an implicit solution method to ensure numerical stability. Then, if melting occurs during the timestep, the conduction solution is repeated to account for the change of phase.

A finite difference formulation in terms of the nodal temperatures is used to model the thermal response of an upper plenum structure. Using the nomenclature defined in Figure A-2, the energy/ conduction equation for the first node (left side of Figure A-2) is:

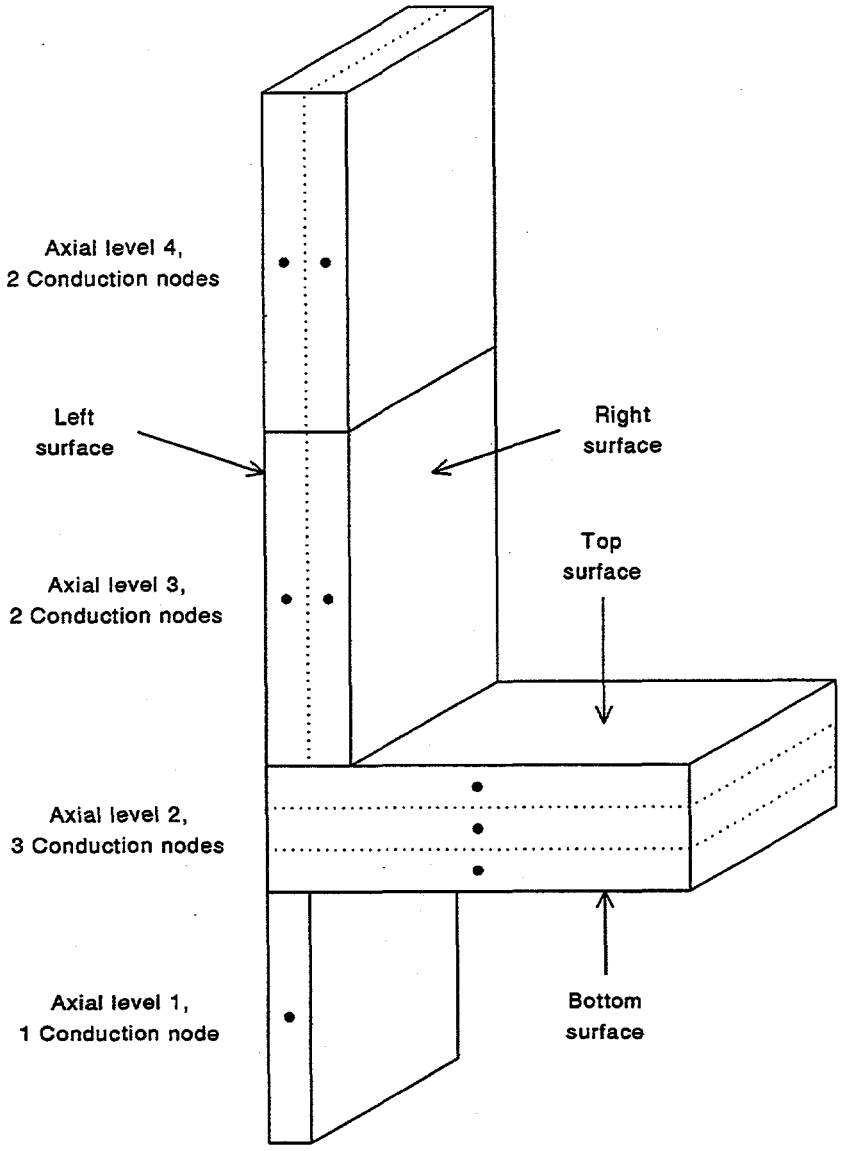

Figure A-1. UPS model terminology for example configuration with 4 axial levels.

$$MC1(TS1_{new} - TS1_{old}) = \frac{TCL - TS1_{new}}{RC1} + \frac{TS2_{new} - TS1_{new}}{R12} + QOL + QSL \qquad \text{(A-1)}$$

When similar finite difference equations are written for the other nodes, they form a linear system of algebraic equations with a tridiagonal arrangement:

TS1, TS2, TS3 = Structure temperatures

TCL, TCR = Coolant temperatures

MC1, MC2, MC3 = Thermal masses (mass times specific heat) divided by timestep

RC1, R12, R23, R3C = Thermal resistances

QOL, QSL, QOR, QSR = Heat transfer rates from oxidation and solidification

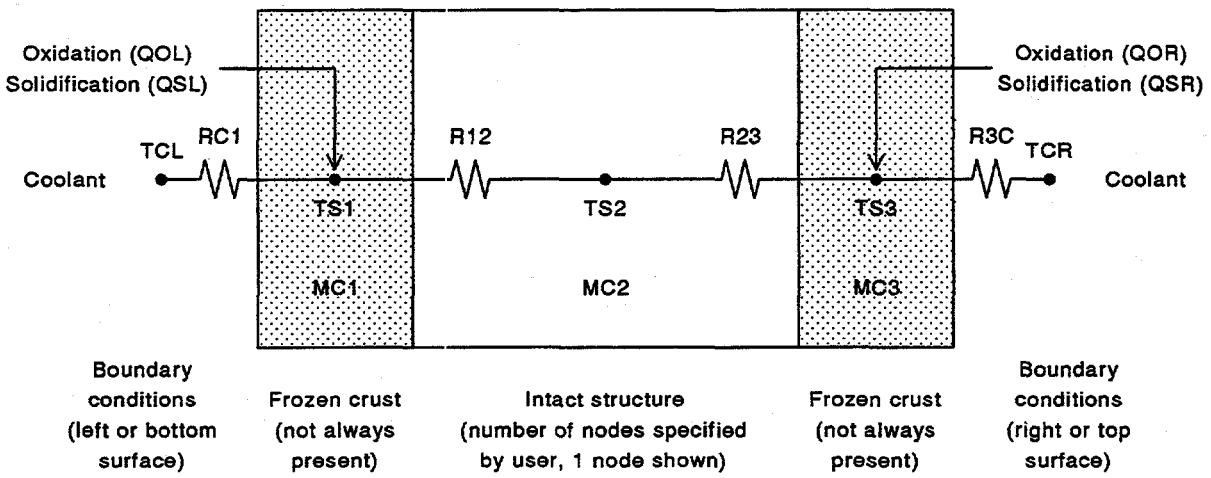

Figure A-2. Nomenclature for solution of 1-D heat conduction equation at each axial level.

$$\begin{bmatrix} MC1+\frac{1}{R12}+\frac{1}{RC1} & -\frac{1}{R12} & 0 \\ -\frac{1}{R12} & MC1+\frac{1}{R12}+\frac{1}{R23} & -\frac{1}{R23} \\ 0 & -\frac{1}{R23} & MC3+\frac{1}{R23}+\frac{1}{R3C} \end{bmatrix} \begin{bmatrix} TS1_{new} \\ TS2_{new} \\ TS3_{new} \end{bmatrix} = \begin{bmatrix} MC1\ TS1+\frac{TCL}{RC1}+QOL+QSL \\ MC2+TS2_{old} \\ MC3\ TS3_{old}+\frac{TCR}{R3C}+QOR+QSR \end{bmatrix} \quad \text{(A-2)}$$

Material properties (specific heat, etc.) for the matrix elements are obtained from the MATPRO library. The nodal temperatures at a new time ($TS1_{new}$, etc.) are calculated simultaneously from the temperatures at the previous time ($TS1_{old}$, etc.) using standard matrix methods.

The implicit solution method for the conduction equation involves a single iteration during a timestep to account for any melting. The temperatures of the boundary nodes at a new time are compared with the melting temperature of stainless steel. If the new temperature of a boundary node is greater than the melting temperature, then that node is removed from the calculation and treated as a constant-temperature conduction boundary condition for the adjacent node. For example, if the above matrix solution predicts $TS1_{new} > TS1_{melt}$, then the first equation is removed from the matrix and $TS1_{new} = TS1_{melt}$ for the second equation:

$$\begin{bmatrix} MC2 + \frac{1}{R12} + \frac{1}{R23} & -\frac{1}{R23} \\ -\frac{1}{R23} & MC3 + \frac{1}{R23} + \frac{1}{R3C} \end{bmatrix} \begin{bmatrix} TS2_{new} \\ TS3_{new} \end{bmatrix} = \begin{bmatrix} MC2\ TS2_{old} + \frac{TS1_{melt}}{R12} \\ MC3\ TS3_{OLD} + \frac{TCR}{R3C} + QOR + QSR \end{bmatrix} \quad \text{(A-3)}$$

The implicit solution for the timestep is then repeated to determine the new temperatures of the remaining nodes. The conduction/energy equation for the melting boundary node is used to determine the melting heat transfer rate:

$$QMELT - \frac{TCL - TS1_{melt}}{RC1} + \frac{TS2_{new} - TS1_{melt}}{R12} + QOL + QSL - MC1(TS1_{melt} - TS1_{old}) \quad \text{(A-4)}$$

and, correspondingly, the mass of stainless steel that melts during the timestep.

The melting temperature of stainless steel oxides is greater than the melting temperature of the pure metal. In the UPS model, the stainless steel oxides do not melt, but rather are carried away as a solid with the pure metal as it melts. The mass ratio of oxides carried away with molten metal is 0.5.

The implicit matrix solution of the energy/conduction equation described in this section is implemented in the UPS model for a user-defined number of conduction nodes at each axial level. When all of the stainless steel in a node melts and relocates downward, that node is removed from the solution. When all of the nodes at an axial level melt, the structure at that axial level is removed from the solution and no longer interacts through convective heat transfer and oxidation with the adjoining RELAP5 hydraulic volumes. It is assumed that all portions of a structure located above an axial level that is completely melted are supported from the side or above and do not collapse downward.

A3 Relocation and Solidification Logic

While it is recognized that PWR or BWR upper plenum structures should begin melting at the lowest axial level and that the resulting molten material would relocate downward directly into the core region, the design report EGG-RAAM-11500[A-1] recommends a more generalized relocation and solidification formulation. Accordingly, the UPS model allows for possible freezing of molten stainless steel on the surfaces of upper plenum structures and also permits molten stainless steel to run down vertical surfaces and to collect on horizontal surfaces.

The relocation logic depends on the surface orientation at an axial level and can be explained with the aid of Figure A-3, which shows a sketch of the possible relocation paths. For a vertical orientation, molten material moves downward along both the left and right surfaces (path 1). A momentum equation is not solved for this downward movement; this material is instead assumed to flow at a constant velocity of 0.5 m/s. Molten material that does not solidify at the lowest axial level of a structure relocates below the defined structure (path 2).

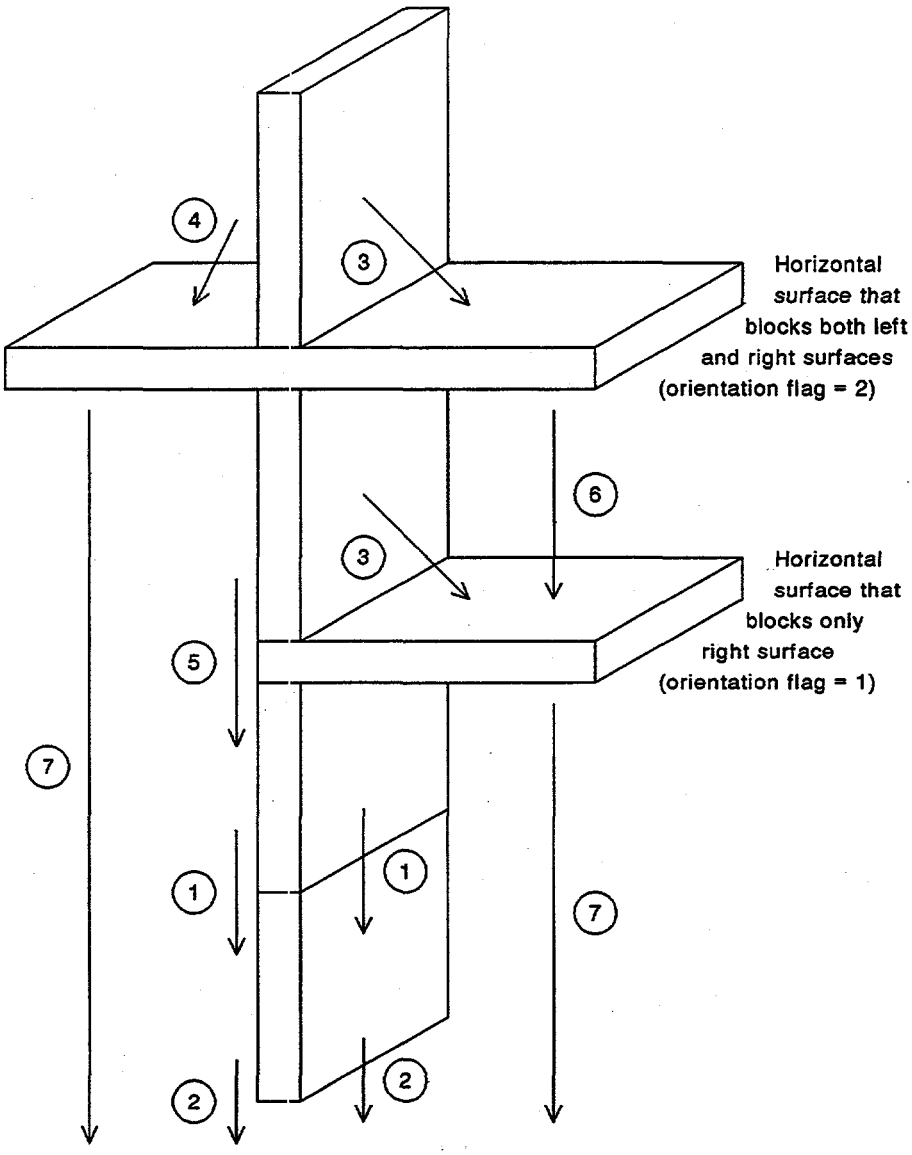

Figure A-3. UPS model relocation logic.

A horizontal surface can block molten material that relocates from an overhead vertical surface. There are two types of horizontal surfaces depending on a user specified orientation flag (see Figure A-3). Both types of horizontal surfaces block relocation from a right surface (path 3). One type of horizontal surface also blocks relocation from a left surface (path 4) while the other type does not block relocation from a left surface (path 5). Whenever a horizontal surface blocks relocation, molten material accumulates on its top surface, where it remains until the entire structure at that axial level melts. Molten material from the top or bottom surfaces of a horizontal structure falls freely until it either reaches the next intact horizontal surface (path 6) or relocates below the defined structure (path 7).

The solidification logic allows molten material to transfer heat to and freeze on the left and right surfaces of a vertical structure and the top surface of a horizontal structure. At the beginning of each timestep (before the 1-D conduction solution described in Section A2), solidification heat transfer rates

from any molten material to the underlying surfaces (variables QSL and QSR in Figure A-2) are calculated at each axial level from (1) a heat transfer coefficient, (2) the surface areas of the molten material, and (3) the temperature differences between the molten material and the surface nodes. The heat transfer coefficient used in the UPS model (estimated by assuming pure conduction in the thermal boundary layer) is 17,000 W/(m^2·K). The surface areas of the molten material may be less than the surface areas of the structure because a layer of molten material is assumed to have a minimum thickness of 0.002 m to account for rivulet flow.

The solidification heat transfer rates are applied as boundary conditions in the energy/conduction equation and are also used to determine the mass of molten material that solidifies during a timestep. The solidification calculations include logic to create new crust nodes (refer to Figure A-1) when the original intact nodes have not begun to melt or have partially melted and then refilled with frozen material.

A4 Oxidation of Stainless Steel

The oxidation logic for the UPS model, which has been adapted from the BWR control blade/ channel box component, accounts for oxidation of stainless steel with a chemical composition of 74% Fe, 18% Cr, and 8% Ni. At the beginning of each timestep (before the 1-D conduction solution described in Section A2), oxidation heat generation rates (variables QOL and QOR in Figure A-2) are calculated at each axial level. These heat generation rates (Cr is an important contributor to these heats of reaction) are applied as boundary conditions in the energy/conduction equation. Steam consumption and hydrogen generation rates are also calculated. The reaction rates are calculated from oxidation kinetics correlations and are limited by the amounts of steam and stainless steel available for reaction.

Three oxidation kinetics correlations are provided for steam-rich, hydrogen-excess, and steam-lean coolant conditions. The applicable correlation is determined using Baker's criteria[A-2] based on the partial pressures of steam and hydrogen present in the coolant. Different combinations of oxide species (FeO, Fe_3O_4, Cr_2O_3, and NiO) are generated for each of these three coolant conditions. The oxidation correlations used for the three coolant conditions are described below.

For steam-rich conditions, White's kinetics correlation[A-2,A-3] is used. The essential chemical reactions for these conditions are:

$$2Cr + 3H_2O \rightarrow Cr_2O_3 + 3H_2$$
$$3Fe + 4H_2O \rightarrow Fe_3O_4 + 4H_2$$
$$Ni + H_2O \rightarrow NiO + H_2$$
$$3FeO + H_2O \rightarrow Fe_3O_4 + H_2$$

For hydrogen-excess conditions, Baker's correlation[A-2] is used. Ni does not react under these conditions. The oxidation of stainless steel will form a "spinal" compound:

$$2Cr + Fe + 4H_2O \rightarrow FeO{*}Cr_2O_3 + 4H_2$$

For steam-lean conditions, a mean of the above steam-rich and hydrogen-excess correlations is used. Ni does not react under these conditions. The essential chemical reactions are:

$$2Cr + 3H_2O \rightarrow Cr_2O_3 + 3H_2$$

$$Fe + H_2O \rightarrow FeO + H_2$$

Whenever an upper plenum structure is at a temperature below the melting temperature of stainless steel, the oxidation rate is generally predicted to be limited by the reaction kinetics. However, when the structure begins to melt and the oxide layer is carried away with the molten stainless steel (refer to the discussion in Section A2), the oxidation rate is much higher and is limited only by the availability of steam. If sufficient steam is available, the oxidation heat generation will continue to melt the structure without any outside heat sources.

A5 Hydrodynamic Interface

The interface logic exchanges parameters between SCDAP/RELAP5 and the UPS model that are required for the oxidation and convective heat transfer calculations. The parameters passed to the UPS oxidation calculation at the beginning of each timestep are the partial pressures of steam and hydrogen and the mass flow rate of steam available for oxidation. When the user specifies that several UPS surfaces are adjacent to the same hydraulic volume, then the amount of steam available for oxidation at a surface is partitioned using a surface-area-weighted average for the volume. The parameters returned by the oxidation calculation at the end of each timestep are the hydrogen generation rate and enthalpy. RELAP5 calculates the steam consumption rate from this hydrogen generation rate.

The parameters passed to the UPS convective heat transfer calculation at the beginning of each timestep are the coolant (liquid and vapor) average temperature and average heat transfer coefficient. A SCDAP utility subroutine (HTRC1) is used to calculate the average heat transfer coefficient for several single- and two-phase coolant conditions. The parameters returned by the convective heat transfer calculation to RELAP5 at the end of each timestep are the average heat transfer rate from the wall to the coolant (liquid and vapor) and the vapor mass generation rate at the wall.

The convection boundary conditions are treated implicitly in the 1-D conduction solution described in Section A2. The heat transfer rates from the coolant to the surfaces of an upper plenum structure are calculated simultaneously in the matrix solution from the coolant temperatures (variables TCL and TCR in Figure A-2) and the surface node temperatures. This implicit treatment helps to minimize numerical instabilities, especially when nodal masses become very small because an upper plenum structure is melting, or when coolant temperatures are changing rapidly.

A6 References

A-1.C. M. Allison and S. A. Chavez, *Proposed SCDAP/RELAP5/MOD3.1 Model Additions to Treat the Behavior of Upper Plenum and Core Plate Structures During the Later Phases of a Severe Accident (Draft)*, EGG-RAAM-11500, September 1994.

A-2.L. Baker, Jr., *An Assessment of Existing Data on Zirconium Oxidation Under Hypothetical Accident Conditions in Light Water Reactors*, ANL/LWR/SAF 83-3, Argonne National Laboratory, 1983.

A-3.J. F. White, et al., *Seventh Annual Report - AEC Fuels and Materials Development Program*, GEMP-1004, March 1968.